A new concrete-glulam prefabricated composite wall system: Thermal behaviour, life cycle assessment and structural response

G. Boscato, T. Dalla Mora, F. Peron, S. Russo, P. Romagnoni

www.elsevier.com/locate/jobe

PII: S2352-7102(17)30401-1
DOI: https://doi.org/10.1016/j.jobe.2018.05.027
Reference: JOBE504

To appear in: *Journal of Building Engineering*

Received date: 20 July 2017
Revised date: 26 May 2018
Accepted date: 26 May 2018

Cite this article as: G. Boscato, T. Dalla Mora, F. Peron, S. Russo and P. Romagnoni, A new concrete-glulam prefabricated composite wall system: Thermal behaviour, life cycle assessment and structural response, *Journal of Building Engineering,* https://doi.org/10.1016/j.jobe.2018.05.027

A new concrete-glulam prefabricated composite wall system: thermal behaviour, life cycle assessment and structural response

[a]G. Boscato, [b]T. Dalla Mora, [b]F. Peron, [a]S. Russo, [b]P. Romagnoni

[a]*Laboratory of Strength of Materials, University IUAV di Venezia, via Torino 153A, 30173 Mestre, Venezia, Italy*
[b]*Department of Design and Planning in Complex Environments, University IUAV di Venezia, Dorsoduro 2206, 30135 Venezia, Italy*

Abstract

This study analyses a new hybrid construction system, the CGFP - Concrete Glulam Framed Panel - that merges the two mostly used materials in frame technology. It is a prefabricated composite wall made of a reinforced concrete slab and a glulam frame.

The strength and stiffness of CGFP have been investigated by load-displacements tests and thermal performance was evaluated by means of a hot-box apparatus. Moreover, the environmental impacts of the system are verified defining its Carbon Footprint and Embodied Energy.

The efficacy of the proposed system was validated by experimental and numerical analysis. Mechanical and thermal properties have been evaluated by means of experimental and numerical tests whose results have been compared showing a good agreement. By structural point of view, the strength and the deformation capacity are ensured through the consecutive and interactive structural response between the wood frame and the concrete slab. By the thermal and environmental point of view, thermal resistance obtained with different kind of insulation materials have been analysed and a calculation of the amount of the Carbon Footprint and Embodied Energy was already performed.

The CGFP panel shows a good thermal performance, a low environmental impact respect to similar construction systems and promising structural behaviour.

Keywords: Timber-concrete composite (TCC); Structural behaviour; Thermal behaviour; Life Cycle Assessment (LCA); Prefabrication

1. Introduction

The wood construction system is still one of the best technologies for building, in terms of sustainability, thermal behavior and structural performance. Traditionally in Europe the wood material has been coupled with brickwork or stone. The use of wood was related to the improvement of seismic performance of masonry buildings [1].

This study proposes a new hybrid construction system, the CGFP (Concrete Glulam Framed Panel) that merges the experiences of the two mostly used materials in frame technology, wood and

concrete, investigating the thermo-physical and mechanical properties as well as evaluating its environmental impact from cradle to gate. From the structural point of view, these systems are built by mechanic coupling plane wall and floor prefabricated elements made of wood, wood-based products and reinforced concrete (RC) material as a set of framed timber and RC panel assembled together through mechanical steel connections.

This paper follows previous publications [2, 3] that presented partial results giving a comprehensive paramount of the outcomes of the research carried out in the last 3 years at IUAV University of Venice (Italy), Strength of Materials and Building Physics Laboratories.

After a first overview on the TCC (timber-concrete composite) technology, three topics are addressed in this paper in order to characterize the CGFP: (i) assessment of structural performance of CGFP through experimental, numerical and analytical investigation aimed to characterize the in-plane strength and stiffness of prefabricated composite wall; (ii) evaluation of thermal resistance of CGFP system varying the typology insulation materials; (iii) environmental impact through a calculation of the amount of the Carbon Footprint and Embody Energy.

1.1. State of the art

Timber-concrete composite structure (TCC) has been developed at the beginning of XX century [4], and the study of Muller [5] gives a first contribution in the design of a system of nails and steel braces aimed to connect concrete slab and timber beams.

In the early times the main application of the TCC technology was on bridges, they have been used in USA since 1930s [6], then to Australia and New Zealand (since 1950s) [7, 8] and from 1990s to Europe [9-12]. After a period of disuse of the 2000s, the use of TCC technology is back [13, 14].

The first applications of TCC for the structural rehabilitation concern the existing timber floors strengthened by shear connectors and a thin roof-plate made by concrete [15, 16]. The analyses of timber-concrete slabs were presented in Flach and Schaonborn [17], Crocetti and Flansbjer [18] and

Crocetti et al. [19]; these latter researches focused on the structural effects of prefabricated FRC slab.

Recently, the researchers studied the load-slip behaviour of different type of shear connectors [20, 21, 22]. Many researches have been carried out on different connections of TCC systems focused to improve the stiffness, strength and ductility. The different connection technologies of TCC systems can be subdivided into three categories: discrete, continuous and glued connections. In detail the first group is characterized by the well-known mechanical connections such as nails, screws and dowels 23, 24]. These connections have been implemented using supports (steel spring [25]) and anchorage systems adding steel profiles and plates [26, 27] or varying geometry and orientation (e.g. X-connectors), [28, 29]. The evolution of the connection systems has been introduced by increasing the contact surface of the anchoring elements using steel elements [29, 30]. A further innovation has been introduced by notches cut into the surface of timber elements coupled with steel fasteners [30, 31] or by grooved connection [32].

For the second category, the continuous connection is realized by means metal plates [33]; this solution increases strength and stiffness ensuring also a ductile behaviour.

The third technology, the glued connection, is a promising solution but with application limits: i) the wet glued connections not allow to ensure an adequate thickness of the glue layer [34]; ii) the dry glued connection solves the previous problem but is a technology that cannot be applied to prefabricated structures [35, 36].

Few researches proposed and analysed the technology constituted by prefabricated concrete slab connected to timber beams which allows to improve the building phase of TCC structures [37, 38].

Through the study on timber-concrete composite bridges the development of test methods for shear connectors have been dealt by Jutila and Salokangas [39].

Loss et al. [40] addressed the topic of the seismic design of timber building through the direct displacement-based design method. A wide investigation of a composite constructive system was presented by Pozza et al. [41], a typical platform frame reinforced with concrete board is tested.

A survey on the state-of-the-art of timber-concrete composite research in the past and recent years has been given by Yeoh et al. [42] and Rodrigues et al. [43]. The first cited reference discusses about the experimental and numerical investigations performed on connections and beams in both the short- and long-term (at collapse and under sustained load, respectively). The same reference is also related to other aspects related the prefabrication, the influence of concrete properties, fatigue tests, fire resistance, vibrations, and acoustics. The second one focuses on the most significant technological innovations and recent developments in the application of TCC structures to bridge construction enumerating the engineering specificities and the advantages of TCC bridge structural systems. The importance of proper mechanical connection for optimal performance of these structures is also analysed and a thorough description of the connection systems suitable for bridge construction is provided.

In the development of a sustainable building system, in the last decades the energy consumption became the main issue for construction industry, residential and commercial buildings that are responsible for about 40% of the total amount of energy consumption and CO_2 emissions in Europe [44]. In this frame EU commission and National Governments indicates stimulate building sector through the Energy Efficiency Directive 2012/27/EU [45] including several requirements towards nearly zero energy buildings (nZEB) by the year 2020, implementing ambitious targets for energy consumption. Because of these requirements as well as general requirements for increased performances and sustainability, the building sector is experiencing a growing demand for modular, light and strong building elements. The aim is to develop components and elements with high degree of insulation, a long-life time, a low CO_2 emission, a low consumption of raw materials, and an attractive surface with minimum maintenance.

Recently precast industry has developed several TCC structural elements for buildings [42], demonstrating high level of performance not only from the point of view of carrying capacity and stiffness, but also according to acoustic, fire resistance and thermal requirements [46, 47].

Dodoo et al. [48] analyses building with concrete-frame and wood-frame focusing on the energy behavior and life cycle analysis. Results show that a concrete-frame building performs slightly lower space heating demand, because of the high thermal capacity of concrete. However, a wood-frame building has a lower life cycle primary energy balance because wood is a bio-material characterized by low production energy demand.

In the general scenario, the high energy performance of buildings is the major issue, supposing however a contribution to the environmental impact decrease given by the building sector [49].

The state of the art in the research proposes only few detailed researches or case studies that deal with the overall environmental benefits of prefabrication [50], especially about embodied energy savings, given by from waste reduction, and about improved efficiency of material usage. Cole et al [51] for example examined energy and GHG emissions related with the on-site construction of a selection of structural assemblies (wood, steel and concrete).

1.2. Structural performance

For the first issue, the structural stability and the dynamic behaviour of these structures derives essentially by the wall elements [52, 53, 54]; for this reason, in this research the strength, the displacement capacity and the energy dissipation capacity have been experimentally evaluated on full-scale timber framed RC panels [55, 56]. Before the direct displacement-based assessment (DDBA) proposed by Priestley et al. [57] the structural analysis of wall element must be evaluated through load-displacement (F-Δ) method. The results of numerical-experimental simulations have been compared with analytical previsions to demonstrate the robustness of the proposed method to evaluate the structural performances for given failure mechanisms - racking and rocking modes of deformation [58] and the related limit states.

1.3. Thermal performance

Precast timber frame system achieves thermal performance and provide an energy efficiency to buildings because of the thermal properties of materials and the ability to combine the layers in a lightweight construction system. In fact, the thermal conductivity of wood is much less than the conductivity of other structural materials and it is about two- four times lower than the common insulating material [59]. Therefore, timber frame construction offers external walls with high thermal insulation for a relatively slender thickness. Recently, the timber frame industry increases the external wall thickness from around 90mm to 140mm and more adding space for installing more insulation material.

Scientific literature demonstrates the effective thermal efficiency of timber frame construction technology. For example, Ge et al. [60] evaluates the thermal performance of two innovative pre-fabricated wood frame wall systems in comparison with a conventional one through one year's field monitoring on BCIT's Building Envelope Test Facility. In that study the two options are related to the addition of insulation in the internal cavity.

Technology with wooden frame could meet the energy performance requirements for buildings: Mahapatra et al. [61] analysed two eight-story wood framed residential buildings according to the Swedish 2012 passive house standard. In Kildsgaard et al. [62] the technical details of the buildings showed that the building envelope, structure and technical systems have an identical design on both buildings; the lower part of the construction was realized in concrete; while for the second level the cross-laminated wood was used. The U-values of the windows, external walls and roof are less than 10 $W(m^{-2} K^{-1})$, 0.11 $W(m^{-2} K^{-1})$, and 0.075 $W(m^{-2} K^{-1})$, respectively. Outputs demonstrates how the actual specific energy use (40.2 $kWhm^{-2}$ $year^{-1}$) in the Portvakten Söder building meet the requirements of the Swedish building code.

In general light-weight timber-based structures have limited heat capacity, leading to problems with temperature swing and thermal load during the summer period [63]. Moreover, the lack of

thermal mass along with the low U-values can be a risk factor in increasing overheating [64]. Skotnicova et al. [65] presented the outcomes of a comparative study of the thermal performance of the external timber frame walls by using numerical simulations and experimental measurements taken on experimental timber frame passive house during the summer months. Results shows a quite good performance of the light-weight timber frame structure.

1.4. LCA performance

This study applies the LCA method for building construction to calculate the carbon emission. According to International Standards ISO 14040 [66], the study proposes a partial LCA framework focusing on the characteristics of construction, including the scope, the system boundary, analysis inventory, impact assessment, and result interpretation.

CGFP panel presents a hybrid configuration based on a wooden frame structure and a reinforced concrete cover. Research undertook a Life Cycle Assessment (LCA) comparing the performances of a conventional construction method with a selected prefabrication method: about 44% saving in embodied energy could be incurred from the use of precast concrete technology in relation to conventional construction of the same building.

Aye et al. [67] analysed precast reusable building modules giving an evaluation of greenhouse gas emissions and energy needs: the study focused particularly on the embodied energy quantification. The outcomes showed up to 81% saving in terms of embodied energy and up to 51% in terms of mass for prefabricated steel buildings. One more example is given by the study of Frenette et al. [68] comparing five wood-frame exterior walls, using different life cycle impact assessment (LCIA) methods. Also Gerilla et al. [69] evaluated the environmental impacts generated by two types of construction, showing how constructions made by steel reinforced concrete (SRC) reveal higher environmental impact compared with wooden residential buildings.

By literature review, Pérez-García et al. [70] showed the environmental benefits given by the Multilayer Structural Panels technology in the construction of low rise residential buildings,

presenting also the evaluation of the economic cost, the embodied energy and the amount of CO_2 emissions during the construction phase.

Martins [71] developed and analyzed a new high performance timber–concrete composite (TCC) panel appropriate for structural applications in floors: TCC panel is environmentally friendly and combines low production and construction costs. In fact, the prefabrication strategy affords improved environmental performance for building construction and the approach of life-cycle assessment gives the possibility to evaluate the main impacts of different phases: pre-production, production, assembly, use, and end of life phases.

1.5. Scope

The researches previously presented allow to contextualize the technology proposed in this paper with respect to structural characterization, thermal performance and environmental impact. The structural response of concrete-glulam prefabricated composite wall which constitutes the new system investigated by analytical experimental and numerical load-displacements tests. Specifically, the wood frame-concrete slab interaction has been experimentally identified to calculate the τ-slip constitutive law in order to update the finite element model and to simulate the structural performances of composite wall system.

The thermal resistance obtained with different insulation materials have been analysed by experimental tests carried out by hot-box apparatus.

The innovative CFGP has been evaluated considering the sustainability through the Life Cycle Assessment (LCA). It is an analysis strategy that considers life cycle of products of process thinking to environmental impacts from production to dismission (cradle to grave).

2. CGFP system general description

The characteristics of CGFP specimens are widely descripted in Boscato et al. [2, 3] and reported in detail in Figure 1. The different types shown in Figure 2 have been tested. In detail: Type A,

length 120 cm; Type B, length 120 cm with door opening; Type C, length 120 cm with window open; Types D and E of 60 cm and 40 cm length respectively.

In detail the concrete framed panel is composed essentially of two parts, a slab of reinforced concrete with a thickness of 50 mm connected with special connectors, integrated to the armature, at the timber frame of conifer homogeneous glulam with resistance class GL24h. This frame is formed by two posts of 80mm x 320mm section and by a crosspiece of 300mm depth, same width of the panel and variable height according to the obtained slab.

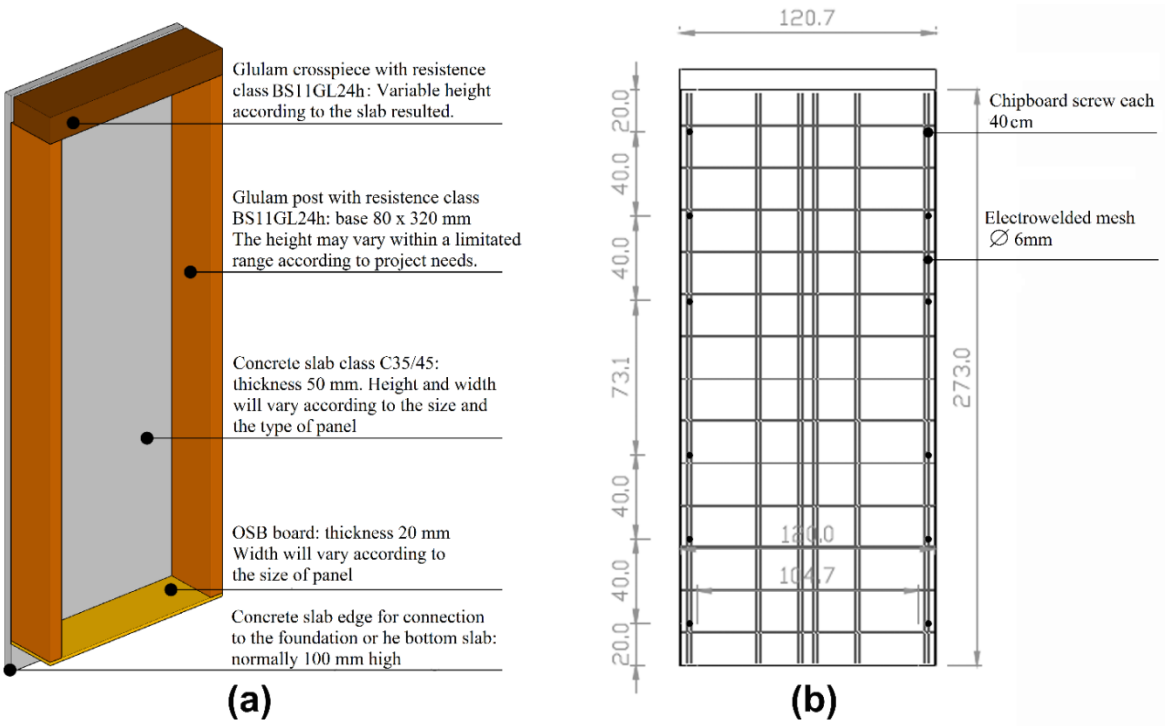

Figure 1. CGFP (Concrete Glulam Framed Panel) standard configuration (a) and electrowelded mesh (b).

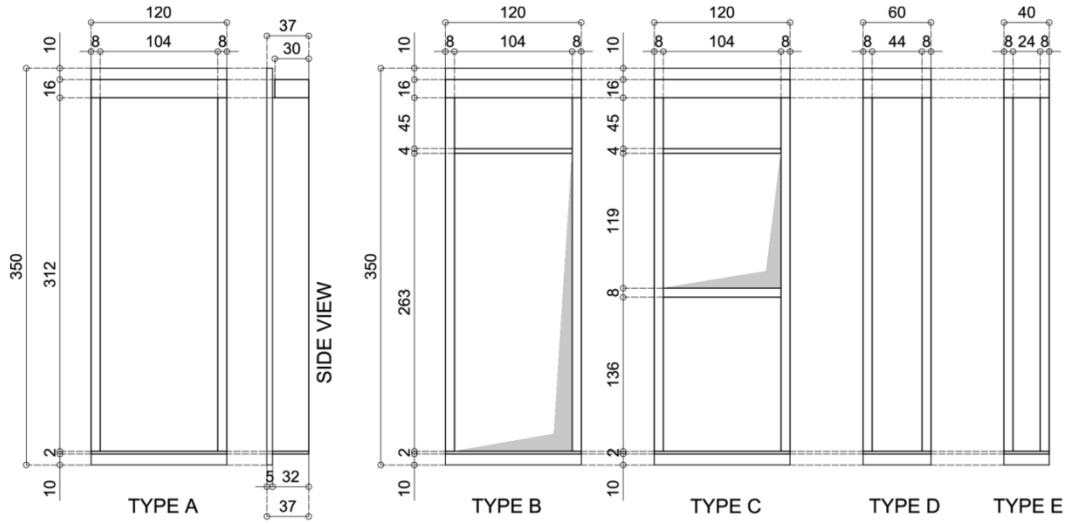

Figure 2. Types of standard panel (dimensions in centimeters).

The assembling phases and the constructive scheme are shown in Figure 3. In detail the building made of CGF panels for load-bearing walls and floors is a modular system where, according to architectural and structural requirements, all the panels are prefabricated. For each panel an innovative type of connection enables the manufacture of the reinforced concrete slab, with a special designed mesh, separately from the laminated wood frame. The individual panels are then assembled providing insulation inside the frames and then are easily transported to the site thanks to their small size. In the ground, after having set up a foundation curb, the panels are hooked to each others with nails and screws. Once all the modules are assembled the construction ends with the plant, doors, windows and interior and exterior finishes.

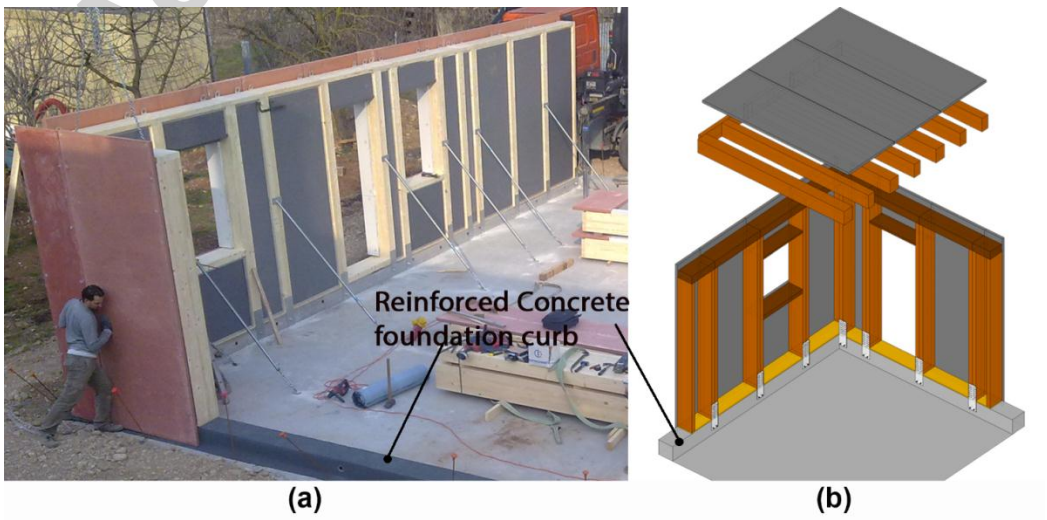

Figure 3. Construction system, (a) assembling phase and (b) 3D scheme.

3. Theoretical and experimental analysis

3.1. Structural performance of CGFP

The performance mechanisms of CGFP is analytically difficult to define. The failure mechanisms should involve the local strength of material and the sliding modes of the connections at the base and between the wood frame and RC panel. The structural performance can be estimated a priori through a simple rigid body respect to in-plane displacement and rotational equilibrium (Figure 4) considering R_A and R_B=couple of forces for the moment at the base; F_V =vertical load; F=horizontal load; R_H=opposite force to F; b=width of panel; h=height.

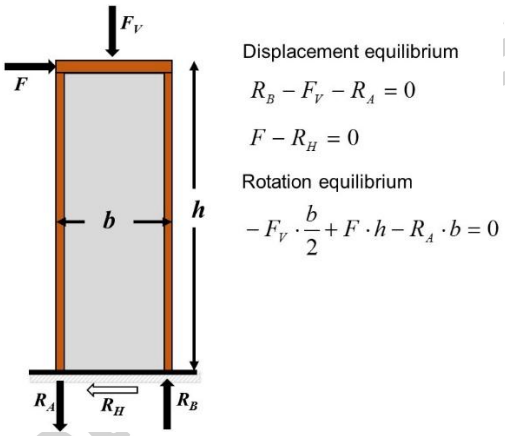

Figure 4. Equilibrium model and equations for a single wall

The most probable mechanism can be evaluated by index S_w as proposed by Loss et al. [58] and developed by equation 1.

$$S_w = \frac{Fh}{\left(R_A + \frac{F_V}{2}\right)b} \quad (1)$$

Each quantity is detailed in Figure 4 and indicated in [3]. When S_w is less than 1 the racking failure mechanism occurs; while when S_w *is* greater than 1 the collapse is due to rocking mechanism. The racking resistance $F_{racking}$ can be asset through equation 2 [72]:

$$F_{racking} = \frac{F_n bc}{s} \quad (2)$$

where F_n is the strength of the connectors, b is the wall panel width, s is the distance between fasteners, c is the reduction factor that is equal to 1 when $b<(h/2)$ or equal to $b/(h/2)$ when $b>(h/2)$.

The rocking mode of deformation mechanism can be calculated by equation 3:

$$F_{rocking} = \frac{\left(R_A + \frac{F_V}{2}\right)b}{b} \quad (3)$$

The top displacement Δ can be calculated by equation 4 [58]:

$$\Delta = \frac{Fh}{Gbt} + \frac{2Fh^3}{(3EAb^2)} + \frac{\delta\left(\frac{h}{l}\right)\left(4\sqrt{2}\cos\phi\right)}{\cos 2\phi} + \frac{(\delta_c + \delta_t)h}{b} \quad (4)$$

Where for the b, h and F see Figure 4. Considering the Equations 2 and 3 the value F can be assumed as $F_{racking}$ or $F_{rocking}$ obtaining Δ_1 (Eq. 5) and Δ_2 (Eq. 6) respectively; E is the elastic modulus of timber, A is the stud cross-section, G is the shear modulus of RC panel, t and l are the thickness and the diagonal length respectively of RC panel, δ is the nail slip, δ_c and δ_t are the vertical displacements at the base of both ends.

$$\Delta_1 = \frac{F_{racking}h}{Gbt} + \frac{2F_{racking}h^3}{(3EAb^2)} + \frac{\delta\left(\frac{h}{l}\right)\left(4\sqrt{2}\cos\phi\right)}{\cos 2\phi} + \frac{(\delta_c + \delta_t)h}{b} \quad (5)$$

$$\Delta_2 = \frac{F_{rocking}h}{Gbt} + \frac{2F_{rocking}h^3}{(3EAb^2)} + \frac{\delta\left(\frac{h}{l}\right)\left(4\sqrt{2}\cos\phi\right)}{\cos 2\phi} + \frac{(\delta_c + \delta_t)h}{b} \quad (6)$$

Table 1 shows the physical and mechanical characteristics of constituent materials given by manufacturer.

Materials	Elastic modulus *E* (MPa)	Shear Modulus *G* (MPa)	Density (kg m^{-3})
Reinforced Concrete (RC)	30960	12900	2400
Wood	E^1 = 14000, E^2=7000	300	650

[1]direction 1 along the development of the structural element, [2]direction 2 transversal to direction 1

Table 1. Physical and mechanical characteristics of materials

The structural interaction between the constitutive components has been characterized by experimental compressive tests carried out on three RC-wood-RC specimens, see Figure 5. The specimens have been assembled by screw Ø12mm and length 160mm, Rothoblass HBS12160 (*Note: all the references are made to a manufacturer's product for the purposes of factual accuracy. No endorsement is implied*).

Figure 5. RC-wood specimens, scheme and setup.

The trend of three experimental tests and the correspondent constitutive law τ-slip are shown in Figure 6 (a) and (b) respectively. In detail starting from the average of the three load-slip relationships (Figure 6a) the constitutive law τ-slip has been calculated as shown in Figure 6b. τ value has been calculated through the compression load that is divided by the two contact areas (400mm x 80mm x 2) between wood and RC elements (Figure 5); while the slip value has been measured through the sliding between the wood and RC elements.

Analyzing the curves of Figure 6a a first common response of three tests is clear before the peak; for both the stiffness is similar while the strength capacity of test 2 (approximately 30100 N) is greater by 20% than tests 1 and 3 with approximately 24300 N and 25000 N respectively. The softening behavior after the peak triggers the plastic failure mode of dowel-type fastener connection.

The details (c) and (d) of Figure 6 show the failure mechanisms of connectors between RC and wood material components. The detail (e) highlights the plastic failure mode of dowel-type fastener connection.

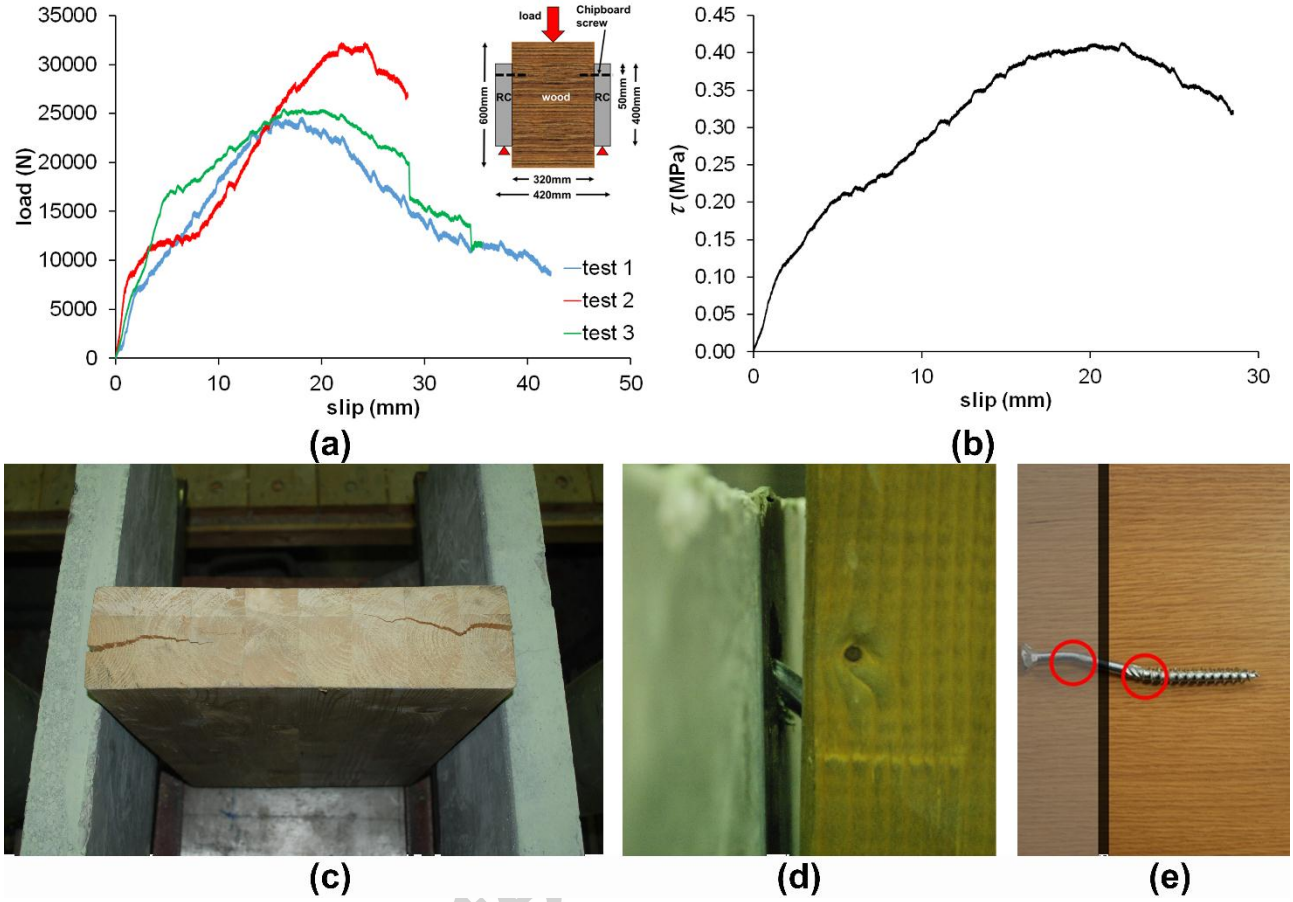

Figure 6. Load-slip curves (a), τ-slip relationship (b), details of failure mechanisms (c), failure mode of dowel-type fastener connections (d and e).

In-plane strength and stiffness have been tested according to UNI EN 594:2011 [73] (Figure 7a), Figure 7b shows the static scheme and the test setup of panel Set 0 (Figure 2). The details c and d of Figure 7 illustrate the applied load (horizontal and vertical) and the base connection respectively.

Uniform vertical load, F_V = 50.4 kN, has been applied to simulate the overhead storey, while the different horizontal load cycles (F) are subdivided in three phases:

(a) stabilizing load cycle with $F = 0.1\ F_{max}$ kept for 120 s and followed by download/recovery phase of 600±300 s;

(b) load cycle for stiffness with $F = 0.4\ F_{max}$ kept for 300 s and followed by download/recovery phase of 600±300 s;

(c) load cycle for strength with $F = 0.4\ F_{max}$ kept for 300 s and followed by download/recovery phase of 600±300 s until reaching F_{max}. $F_{max} = F$ value has been preliminary calculated through equilibrium equations for displacement and rotation.

The experimental test setup is described in Figure 7. The four sets (Figure 8) with different combinations of types shown in Figure 2 have been monitored by instruments according to UNI EN 594:2011 [73].

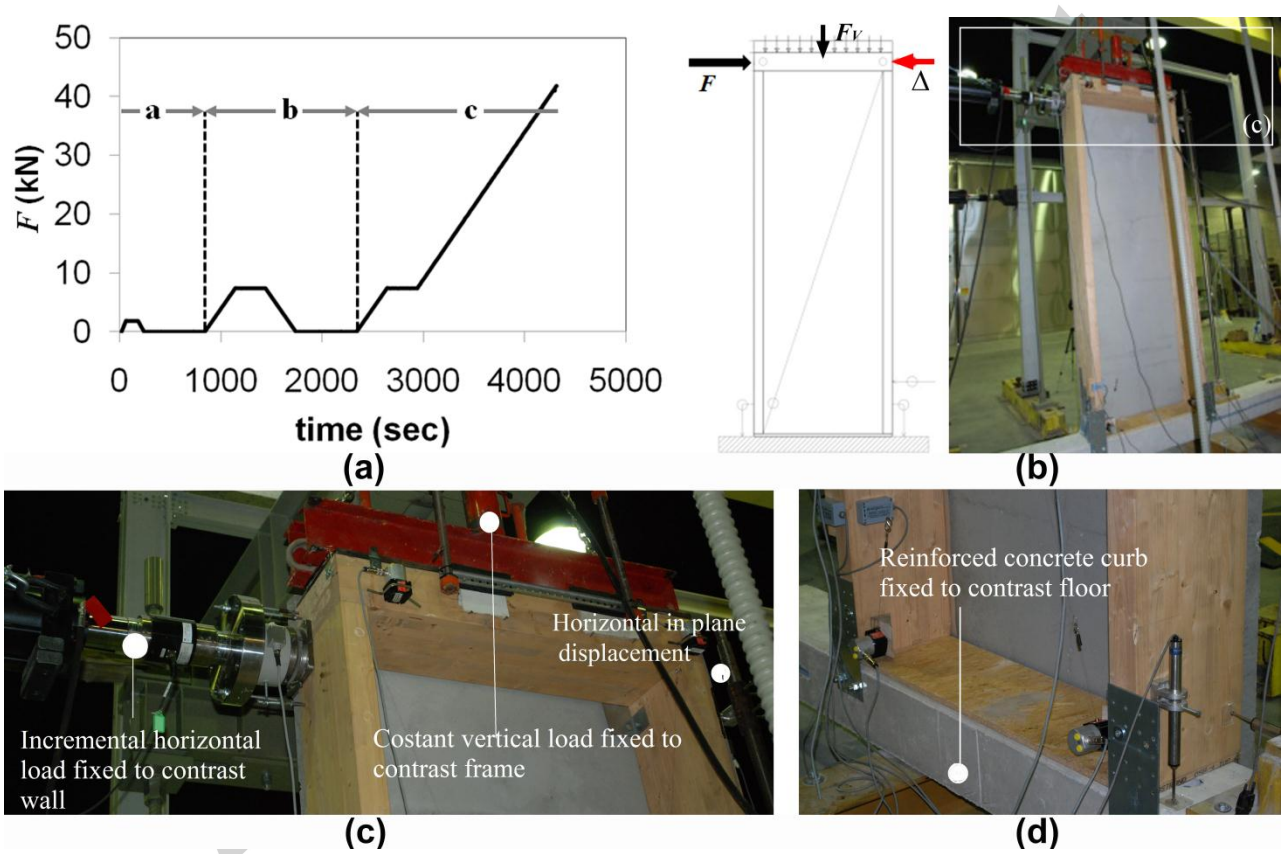

Figure 7. Quasi-Static Ramp Tests (a), setup (b) and details (c and d).

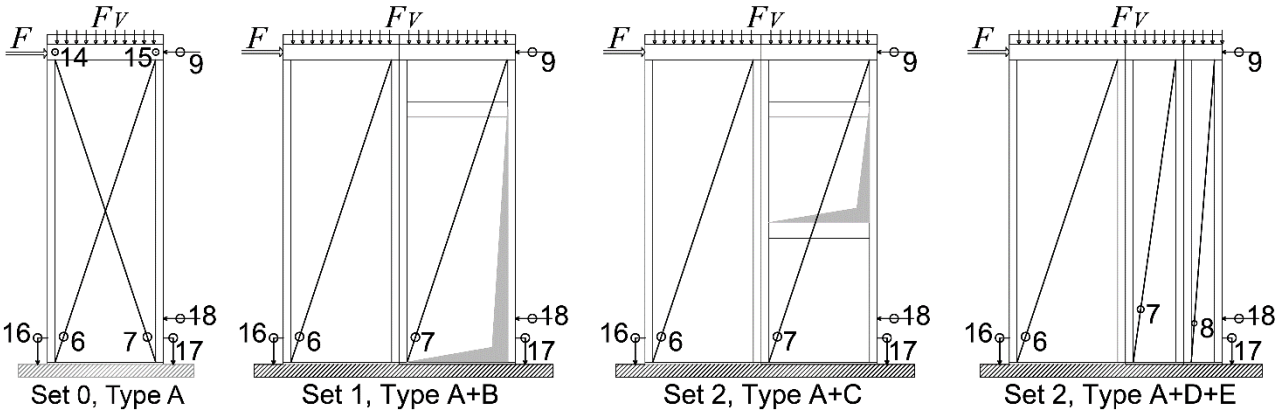

Figure 8. Sets and position of displacement transducers for every test

The horizontal load *F* has been applied by hydraulic actuator (MTS 201). In detail, as shown in Figure 8, the wire displacement transducers 6-7-8 (Micro Epsilon WDS-500-P60-SR-U) measure the diagonal variation, the transducers 9 and 18 (Vishay Micro Measurements HS100) measure the top (Δ) and the bottom displacements, 14 and 15 measure the displacements (wire displacement transducers by Micro Epsilon WDS-500-P60-SR-U) out of plane (only for Set 0) while 16 and 17 measure the vertical displacements of both ends (Vishay Micro Measurements HS100). (*Note: all the references are made to a manufacturer's product for the purposes of factual accuracy. No endorsement is implied*).

Table 2 lists the maximum load and the displacements recorded during the tests by each transducer shown in Figure 8. The values that mark the bi-linear behavior, through the change from linear to non-linear structural response, are given in the brackets. The double brackets of test 2 are due to the last branch of the tri-linear response (see Figure 9a).

Panel	**Load *F* [N]**	**Displacement [mm]**								
		t6	**t7**	**t8**	**t9**	**t14**	**t15**	**t16**	**t17**	**t18**
Set 0, test1	17338	22.1 (15.76)	/	/	73.93 (57.11)	-14 (-27)	22.05 (37)	-2.97 (-1.45)	2.8 (1.99)	3.37 (2.68)
Set 0, test2	21126 (16858)	43 (23) ((15))	/	/	149 (95) ((60))	-21 (-27)	9 (14)	-11 (-5) ((-3))	3 (1) ((0.1))	3 (1) ((0.17))
Set 0, test3	20404	26.9 (15.7)	/	/	93 (62)	-13.93 (-40)	11.15 (25.35)	-4.43 (-2.41)	1.93 (1.19)	0.62 (0.13)
Set 1	30108 (20135)	65.56 (11.02)	19.25 (2.06)	/	60.15 (11.21)	/	/	38.6 (2.15)	7.99 (2.15)	10.03 (1.93)
Set 2	34460 (22142)	15.96 (11.19)	71.22 (41.05)	/	21.84 (12.91)	/	/	7.26 (1.4)	1.95 (0.89)	5.12 (2.49)

Set 3	41738 (24165)	13.6 (5.19)	8.59 (2.23)	4.82 (0.52)	22.75 (6.7)	/	/	11.75 (1.21)	3.01 (1.21)	1.08 (0.4)

Table 2. Maximum load and displacement data, where t is the wire displacement transducer.

The structural response of set 0, Type A, (test 1, 2, 3) is shown in Figure 9a through the load-displacement relationship; while the structural performances of sets 1, 2 and 3 are shown in Figure 9b. The displacements have been recorded by t9 displacement transducer (Figure 8).

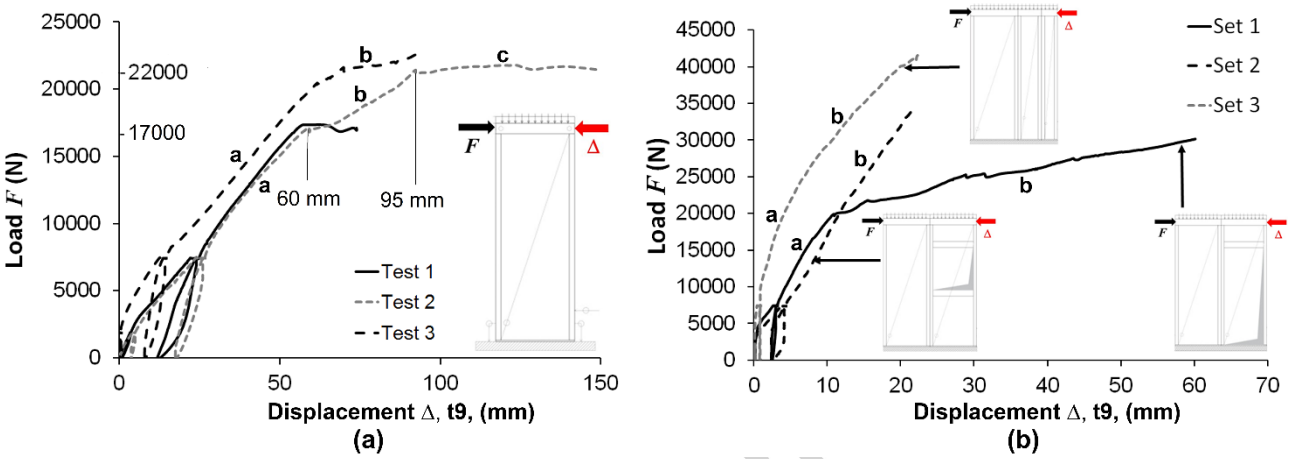

Figure 9. Load-top displacement response: a) Test 1, 2 and 3 for Set 0; b) Set 1, 2 and 3.

Figure 9a highlights the main results both for the strength and for the displacement capacity showing a good agreement between the three tests of Set 0.

The trend of the first branch (a) of all curves confirms the linear behavior until the 17000 N. In detail, Test 1 reaches the collapse to approximately 17000 N; while Tests 2 and 3 show the failure load up to approximately 22000 N. The stiffness of Test 2 changes to approximately 17000 N with the branch (b) up to the failure load to approximately 22000 N with the branch (c).

A dissipative capacity was recorded by Test 2 with tri-linear response through the different grade of consecutive branches (a), (b) and (c).

The structural response of Set 1, 2 and 3 are compared in Figure 9b.

Set 1 and Set 2 have similar linear behavior up to approximately 21000 N (branch (a)) with a displacement of approximately 11 mm, the bifurcation is due to the different effect of panel Type B (panel with door, Figure 2) and C (panel with window, Figure 2) on panel Type A (Figure 2). In the

configuration Set 2 the panel with window (Type C, Figure 2) has in-plane stiffness like panel Type A ensuring almost a global linear behavior; in the Set 1 the in-plane lower stiffness of the panel with door (Type B, Figure 2) causes a non-linear global behavior and a consequent dissipative capacity as shown by the grade of branch (b), see Figure 9b. The behavior of Set 3 is characterized by the greater stiffness than Set 1 and 2 offered through the in-plane structural interaction of the wall panels without openings, Types A+C+D.

For the panels of Set 0 the failure mechanisms involve mainly the link at the base, with local damage (Figure 10a, b, d, e, g, h), and the bracing role of RC panel with flexural behavior followed by in-plane shear collapse (Figures 10b, c, f, i).

For the Sets 1, 2, and 3, the failure mechanisms are shown in Figure 11; the collapse was activated by the local mechanism at the base, in the joint between RC slab and curb (Figure 11b, c, e, h). Set 2 and Set 3 triggers the rocking mechanism involving the local collapse between the RC slabs (Figure 11, details f and i). From the point of view of the failure mechanisms Set 1 behaves like the panels of Set 0, without the interaction between the bracing panel and affecting only the local connection panel-curb.

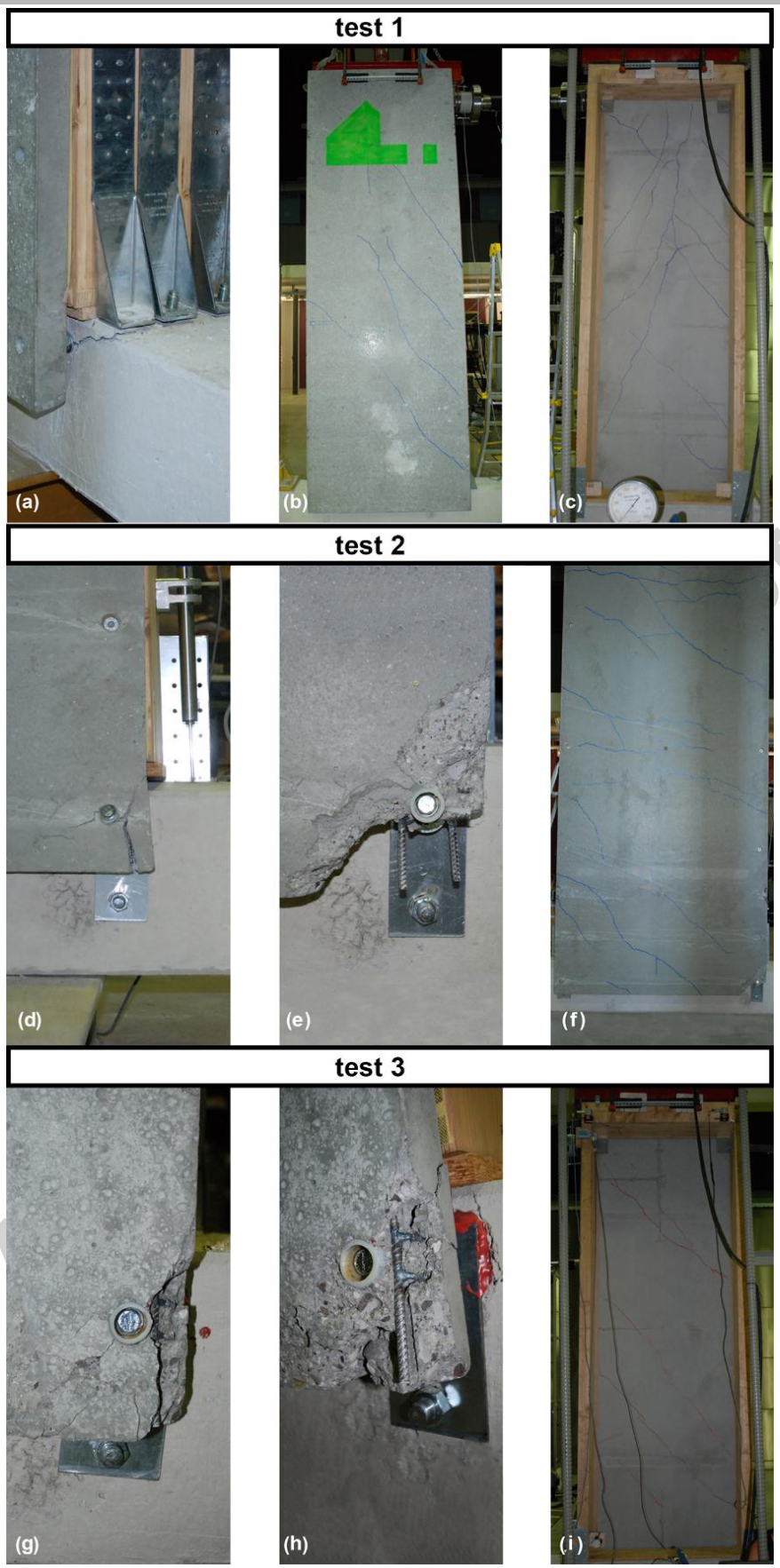

Figure 10. Failure mechanisms of panels Set 0.

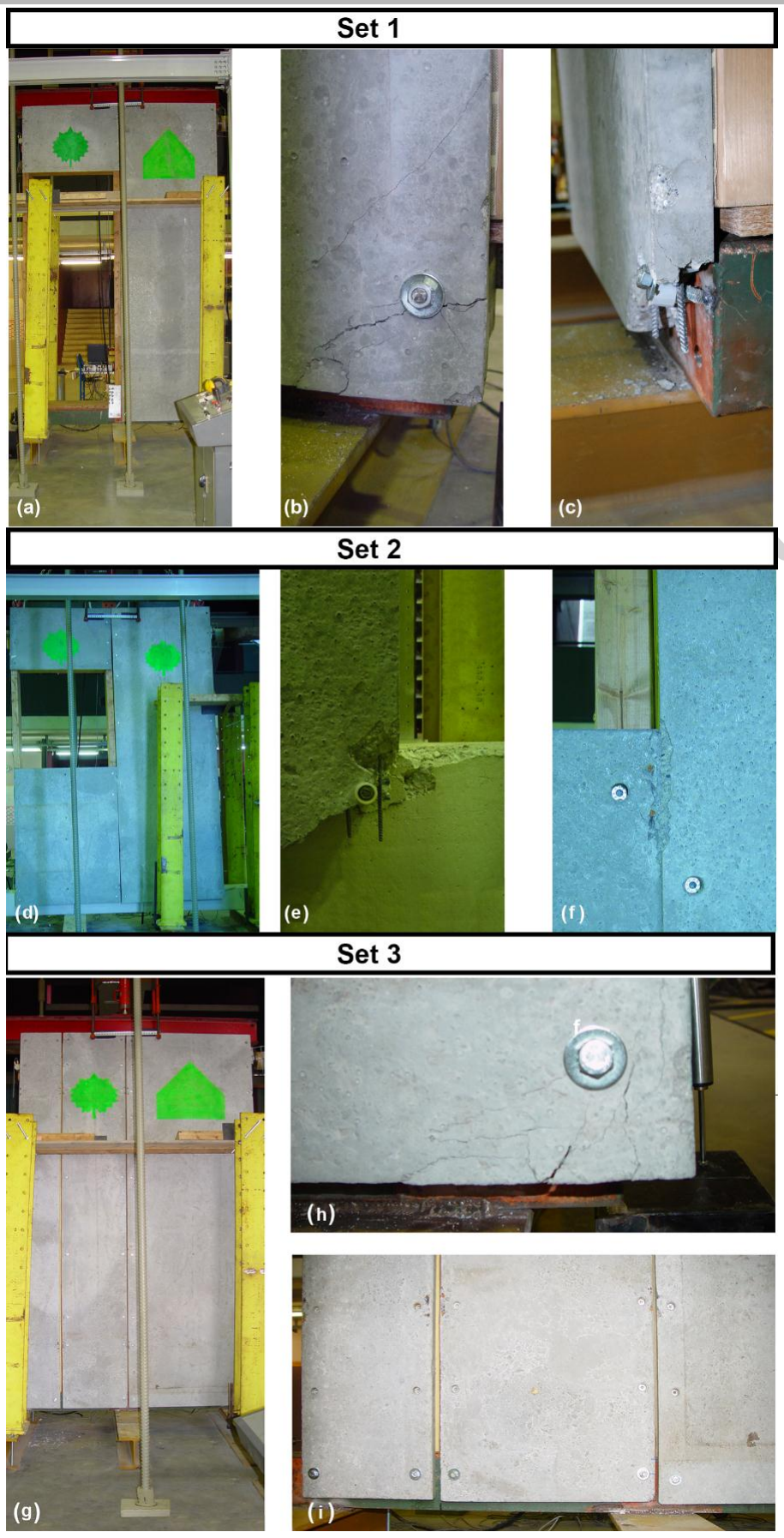

Figure 11. Failure mechanisms of panel Set 1, 2 and 3.

The response of a single panel and the structural interaction between the different configurations are affected by failure mechanism of components with the relative behaviour of the shear wall. The triggered racking and rocking modes of deformation develop a ductile behaviour through the elastic response, due to progressive deformation of structural members and connectors, and inelastic one following connector yield [57], Figure 6 d and e. The combination of both failure mechanisms depends by: a) racking mode due to sliding between the sheathing RC panel and the wood frame (Figure 10, details b, f and i); b) rocking mode activated by the failure of the base anchoring (Figure 10, details a, e and g).

3.2. Thermal Experimental analysis

Experimental tests have been carried out in order to evaluate the energy performance using an hot-box with reference to the standard UNI EN ISO 8990 [74, 75]. The standard prototype, insulated with polystyrene foam, was characterized in two different configurations which correspond to possible field application conditions. The first one had a ventilated air gap between the concrete slab and the insulation layer while in the second configuration the outside air gap was non-ventilated (Figure 12).

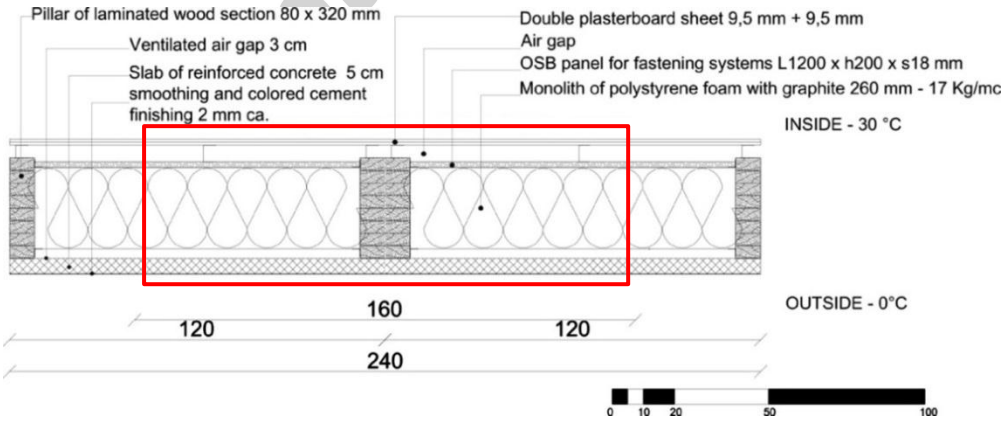

Figure 12. Section through a panel of type A. Red box describes the area analysed in the hot-box apparatus. Dimensions in centimetres.

For each configuration two tests have been performed, measuring the thermal transmittance in two sections: through the wooden pillar and through the insulation panel. In the first configuration the air temperature difference between the two sides of the specimen has been measured 29.6°C and

the thermal transmittance values were respectively 0.20 W m^{-2} K^{-1} and 0.19 W m^{-2} K^{-1}, converged to the average value of 0.195 W m^{-2} K^{-1}. In the second configuration the difference of the air temperature was of 29.4°C and the transmittance value was 0.19 W m^{-2} K^{-1}. As expected the transmittance outcomes give the same values, due to the not-great relevance of concrete slab in term of thermal resistance.

4. FEM analysis

With the aim to extend the experimental results, a numerical analysis has been carried out in structural and thermal fields by commercial Strand 7 code [76]. For the structural analysis the finite element (FE) model of the single panel (Set 0) has been updated considering the load-displacement relationships of Figure 5a; the non-linear solution was conducted by using the code's non-linear static solver (http://www.strand7.com/html/nonlinearstatic.htm). The thermal response the thermos-physic properties of the materials were set up in the FE model in order to identify the thermal bridge between the assembled parts. The steady state heat solver is used to calculate the temperature distribution in a structure in the steady state or equilibrium condition by using the code's steady state solver (http://www.strand7.com/html/steadystateheat.htm).

4.1. Mechanical numerical analysis

The panel has been modelled by 2464 brick elements. The assumed boundary conditions are shown in Figure 13, while the material properties are listed in Table 1.

In detail the numerical model of RC material has been characterized considering the isotropic behavior; while the wood material has been modeled with orthotropic behavior, anisotropic along the fibers (direction along the development of element) and transversally isotropic behavior. The FE model has been fixed at the base leaving free the rotation around Z (RZ) and restrained at the top in Z direction (DZ, see Figure 13) in order to avoid the out-of-plane displacements.

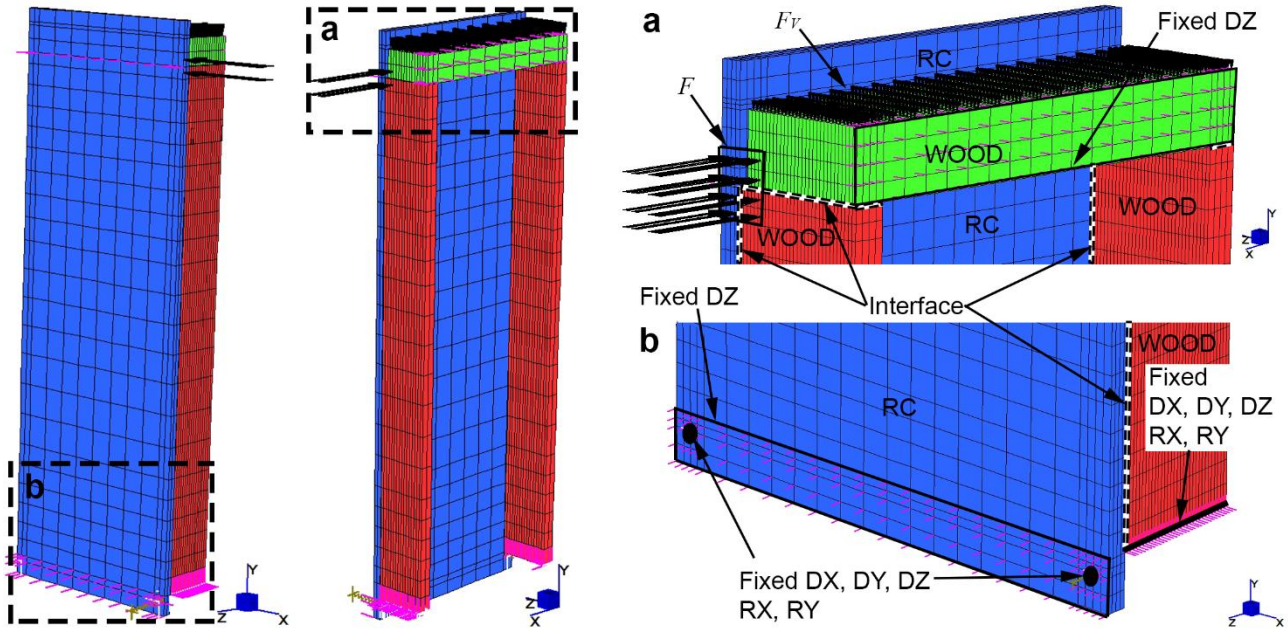

Figure 13. Details and boundary conditions of Finite Element Model; (a) detail of top of panel Set 0; (b) detail of bottom of panel Set 0

The non-linear static analysis has been carried out through the non-linearity of interface wood frame-RC panel (Figure 13 a and b) realized with bricks with infinitesimal thickness and characterized by the experimental constitutive law τ-slip of Figure 6b.

For the complex Set 1, 2 and 3 the interaction between the different panels, Types A, B, C, D, E, has been realized by the interface (like wood frame-RC panel interface) characterized by the constitutive τ-slip law reported in Figure 6b.

The good reliability of numerical analysis is shown in Figure 14 through the comparison between the experimental and numerical responses (dashed lines).

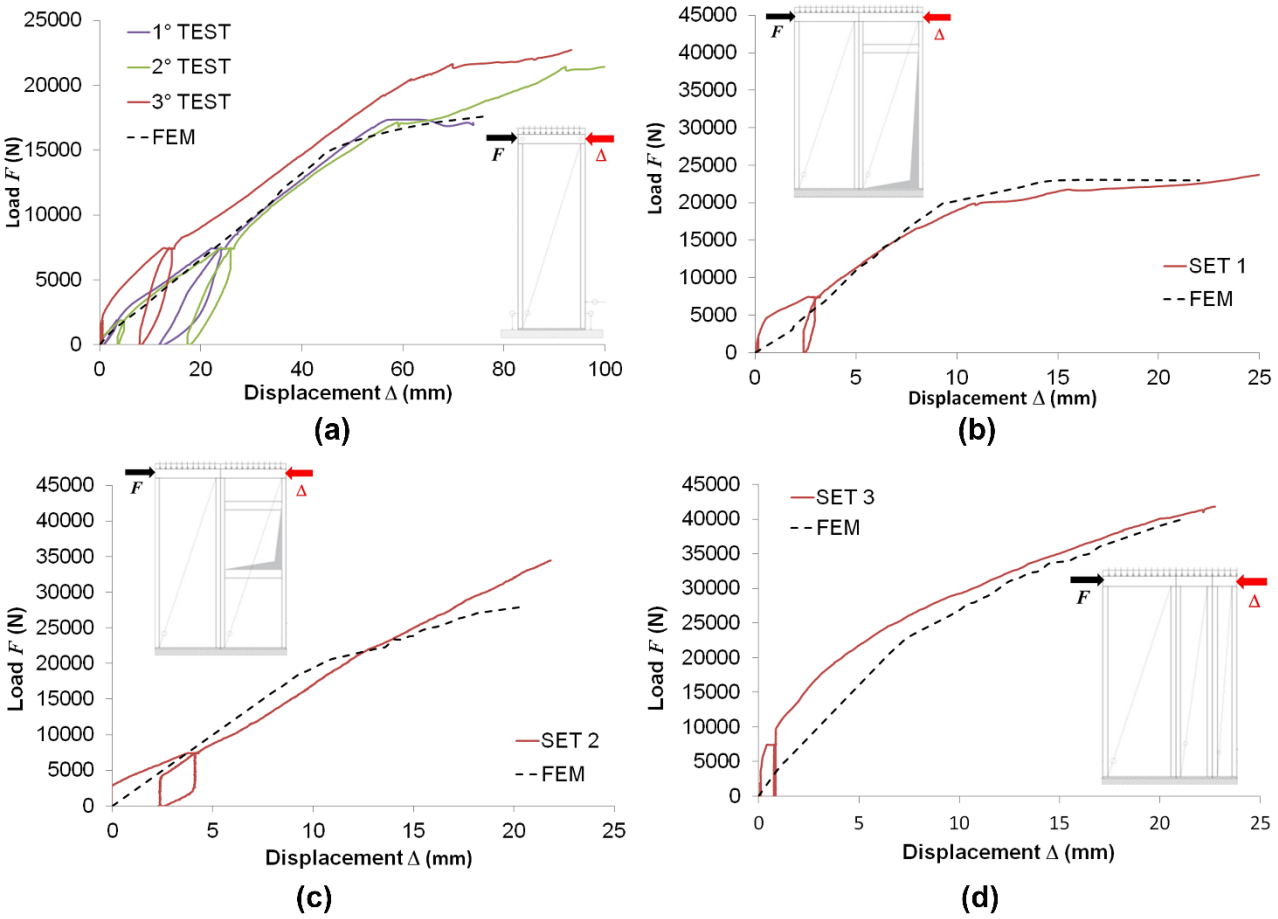

Figure 14. Comparison of experimental and numerical results; (a) Set 0; (b) Set 1; (c) Set 2; (d) Set 3

Through the maximum structural capacity of the panel of Set 0 (test 1, 2 and 3) the reliability of the analytical approach (see paragraph 3.1) is evaluated in Table 3. It compares the experimental (EXP) and numerical (FEM) data with the results calculated through Equations 2, 3 and 5, 6 for the horizontal force and displacement respectively. The coefficient of variation (COV) is calculated between EXP, FEM and analytical data.

Type	**EXP**		**FEM**		**Analytical**				**COV (%)**					
	F	Δ	F_{FEM}	Δ_{FEM}	$F_{racking}$	$F_{rocking}$	Δ_1	Δ_2	F/F_{FEM}	F/F_{Eq2}	F/F_{Eq3}	Δ / Δ_{FEM}	Δ / Δ_1	Δ / Δ_2
	[N]	[mm]	[N]	[mm]	[N] Eq. 2	[N] Eq. 3	[mm] Eq. 5	[mm] Eq. 6						
test 1	17338	73.93							1%	21%	33.8%	3%	68%	70%
test 2	21126	149	17605	76	21942	26200	230	245	17%	3.7%	19%	49%	35%	39%
test 3	20404	93							14%	7%	22%	18%	59%	62%

Table 3. Comparison between experimental (EXP), numerical (FEM) and analytical data of Set 0.

Comparing the values reported in Table 3, it is possible to assert that the analytical approach to evaluate the CGFP panel is reliable for the maximum horizontal load *F*. The better coefficient of variation (COV) between EXP and analytical data of maximum load is with the Racking mechanism approach calculated through Equation 2; in detail, the variation between experimental and analytical data is less than 7% for the tests 2 and 3 while the COV is greater than 21% for test 1. About the maximum displacements Δ, the proposed analytical approaches overestimate the performances of the CGFP panels; in detail, the variation between experimental and analytical results is greater than 35%. The finite element analysis agrees with experimental behaviour for the maximum load; while the displacement values are difficult to simulate. In detail, the variation of maximum load values is between 1% and 17%, while for the displacements the coefficient of variation varies between 3% and 49%. For both quantities, horizontal load and displacement, the numerical results approximate better the experimental values of test 1.

4.2. Thermal numerical analysis

Thermal simulations by FEM allow to obtain the transmittance on glulam frame area and in the middle of panel area. The two values were weight by the areas and a total U-value was calculated. After a tuning process a thermal transmittance of 0.189 W m^{-2} K^{-1} was found: this result is in good agreement with the experimental data (see table 4). After this tuning phase has been possible to investigate the existence of thermal bridges in the structures, obtaining the L^{2D} of different connection typologies.

Specific	Unit	Value
Average heat flux	[W m^{-2}]	5.5
Model area	[m^2]	3.52
Internal temperature	[K]	303.37
External temperature	[K]	273.98
Temperature difference	[K]	29.39
Internal adduction coefficient	[W $m^{-2}K^{-1}$]	8.12
External adduction coefficient	[W $m^{-2}K^{-1}$]	23
Wall transmittance	[W $m^{-2}K^{-1}$]	0.189
Wall resistance	[m^2K/W^{-1}]	5.344

Table 4. Thermal transmittance of FEM model.

The main interfaces between envelope elements have been considered: perimeter wall and vertical coverage connection; vertical perimeter wall and attic; perimeter wall and balcony; corner between two vertical walls. Figure 15 shows the temperature distribution across the structure and the relative linear coefficient- The L^{2D} obtained for the four nodes are respectively 0.50 $Wm^{-1}K^{-1}$, 0.33 $Wm^{-1}K^{-1}$, 0.53 $Wm^{-1}K^{-1}$ and 0.53 $Wm^{-1}K^{-1}$.

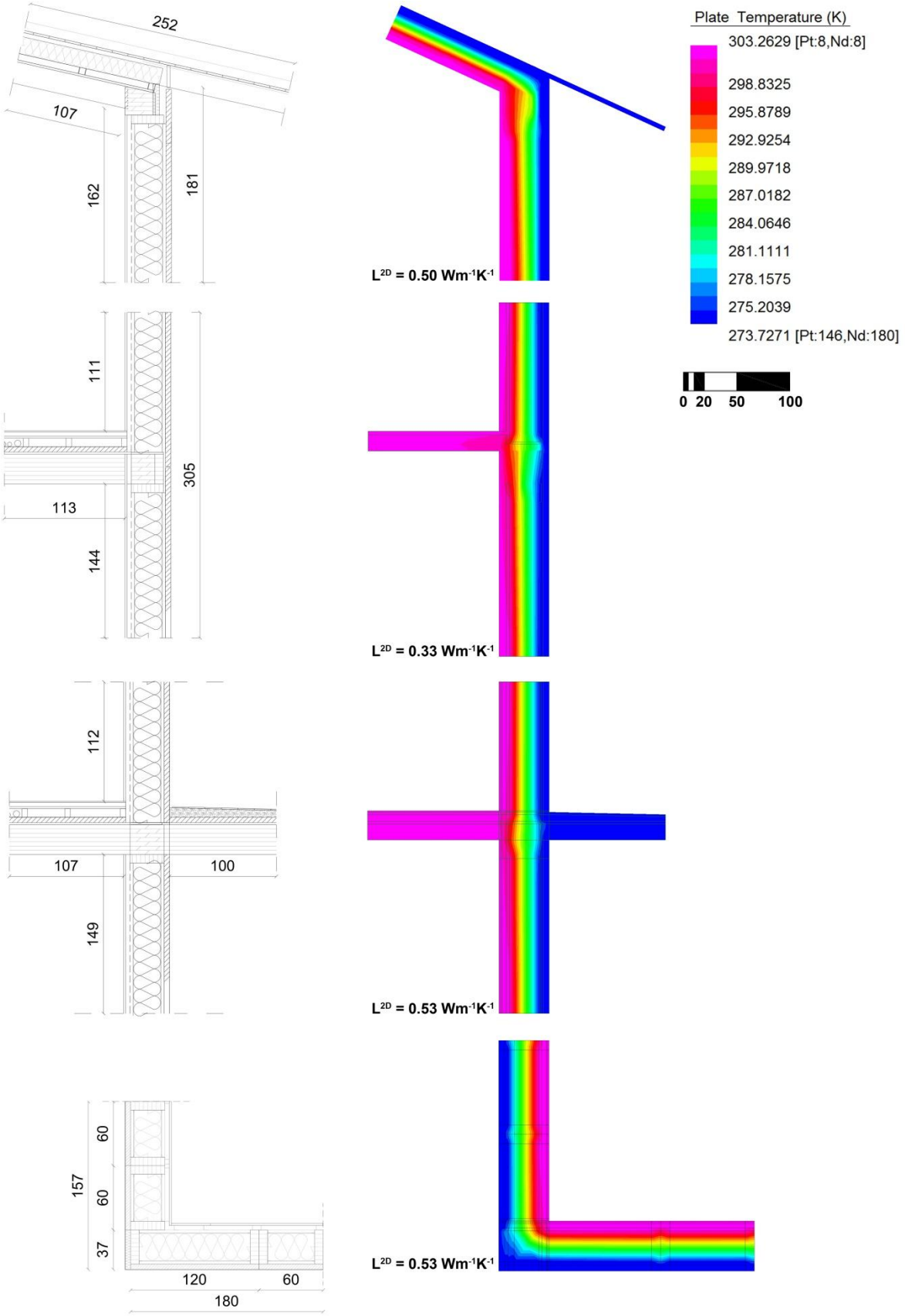

Figure 15 - Thermal bridges analysis in structures realized by panels of Type A, dimensions in centimetres.

5. Life cycle assessment

The LCA study focused on the base configuration of the panel, the so called CGFP-type A; the composition is characterized by a wooden frame supporting a concrete slab insulated by polystyrene foam with graphite.

This study aims to quantify the carbon dioxide emissions and the embodied energy of the modular prefabricated panel for study the amount of the environmental effects of building life cycles and to assess the potential benefits on using different kinds of insulation materials. In this sense the scope is the evaluation of a partial LCA, with a "from cradle to gate" approach (Figure 16) and the system boundary concerns on a definite scenario during a 50 years of building life-span: the facilities and equipment used for the extraction and production of raw materials; the transport and the conversion of the materials into production process; the assembling in factory of each products in order to build the panel; the assessment stops at the factory gate, before the finished product has been transported in site construction.

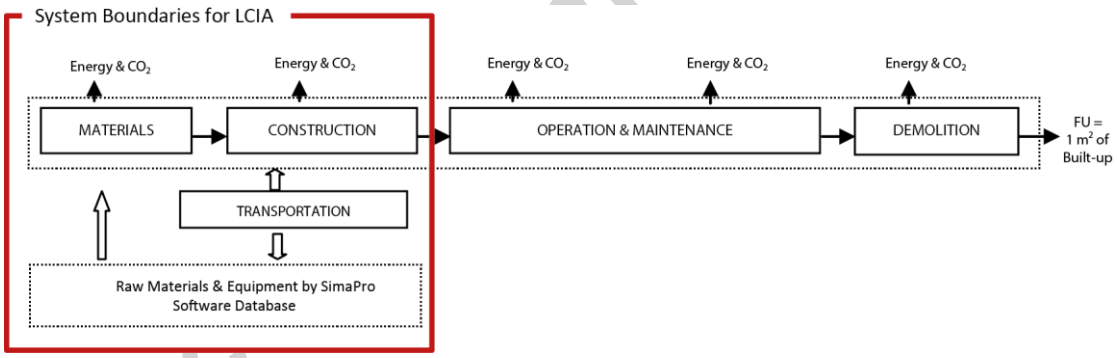

Figure 16. System Boundary for LCIA of CGFP typical configuration.

The fundamental definition of functional unit in life cycle assessment take reference in the ISO 14040:2006 [76] as the quantified performance of a product system for use as a reference unit: all inputs, outputs, and analysis should relate to the functional unit to ensure a comparison between alternative products, processes, or services made on an equivalent basis. In this study the chosen functional unit is 1 m^2 of opaque wall component as a reference for both inventory flows and environmental impacts. The assumed life span of the panels is 50 years with no maintenance

necessary in that period. It was assumed that the panels will be used for construction/retrofitting of buildings located in the area of Treviso (Italy).

Evaluation of impacts along the life cycle for all materials was developed using SimaPro 8.0.5.13 [77], Ecoinvent database v3.2 [78] and analysis method Impact 2002 + [79]. Consequently, the impacts are expressed in points: a composite measure of the overall environmental impact of any material, product or service. A point represents the average impact in a specific category caused by a person during one year in Europe [44]. This study presents values expressed in points per square meters of components surface.

According to LCA framework, the first phase (called Life Cycle Inventory, LCI) aimed to collect all data about the processes and the quantity of each material involved in the production of the panel in term of volume and density, in order to calculate the total weight of each material (Table 5). In the second phase (Life Cycle Impact Assessment, LCIA) each environmental impact was classified.

Material	Volume [m^3]	Density [kg m^{-3}]	Weight [kg]
Double plasterboard sheet	0.0752	800	60.2
OSB Oriented Strand Board panel for fastening systems	0.0374	550	20.57
Monolith of polystyrene foam with graphite	0.8424	17	20.18
Reinforced Concrete, smooth and coloured, finishing 2 mm	0.2100	2400	504
Pillar of laminated wood section 80 x 320 mm	0.1597	418	66.46
Glulam crosspiece	0.0576	520	29.95
OSB Oriented Strand Board: thickness 20 mm width will vary according to the size of panel	0.0077	550	4.235
Aluminium profiles	0.0004	2700	1,08
Polyethylene points (n.22)	0.000065648	1100	0.0721
Profiled iron	0.00075	7800	5.85

Table 5. Characterization of CGFP materials.

The methodology of Impact 2002+ [80] was applied (Figure 17): each impact are characterized in different categories and the characterization factors, CF, for the different categories are based on a principle of equivalence; the assigned scores to the different substances are expressed in kg equivalents of a reference substance (e.g., the Global Warming Potential on a 100 years scale of fossil methane is 27.75 times higher than CO_2, thus its characterization factor is 27.75 kg CO_2-eq).

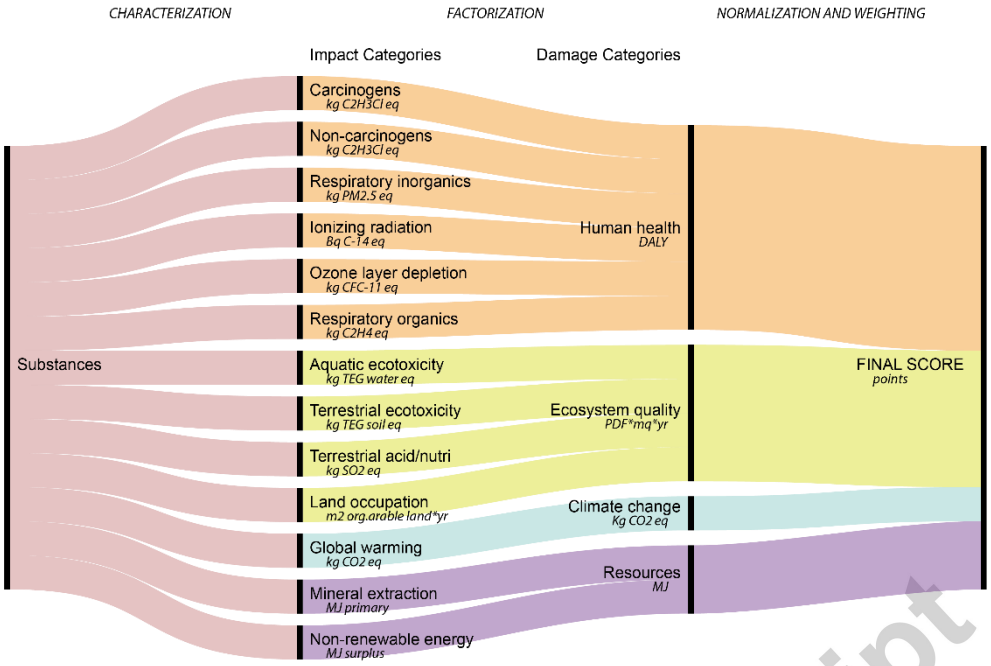

Figure 17. IMPACT 2002+ methodology.

Impacts are organized in four damage categories -human health, ecosystem quality, climate change, and resources- measured by different types of units, and are normalized at least in points.

The main objective, common to all impact categories, lays in the definition of long-term effects, obtained through the use of a time horizon. The comparative analysis of the environmental impact materials was made considering $1m^2$ of surface and a life span of 100 years. The boundaries of the systems are established using an approach from cradle to grave, within the production, installation, cleaning, maintenance and end of life. Within those boundaries the facilities and equipment used for the extraction of raw materials, the transport and the production process were considered. The inventory analysis was conducted using data obtained from the Ecoinvent database v3.2 [78].

In the last phase (Interpretation), processes analysis underlines that Glued laminated timber shows the higher impact, while the other materials and operations have lower ones due to their little amount (Figure 18).

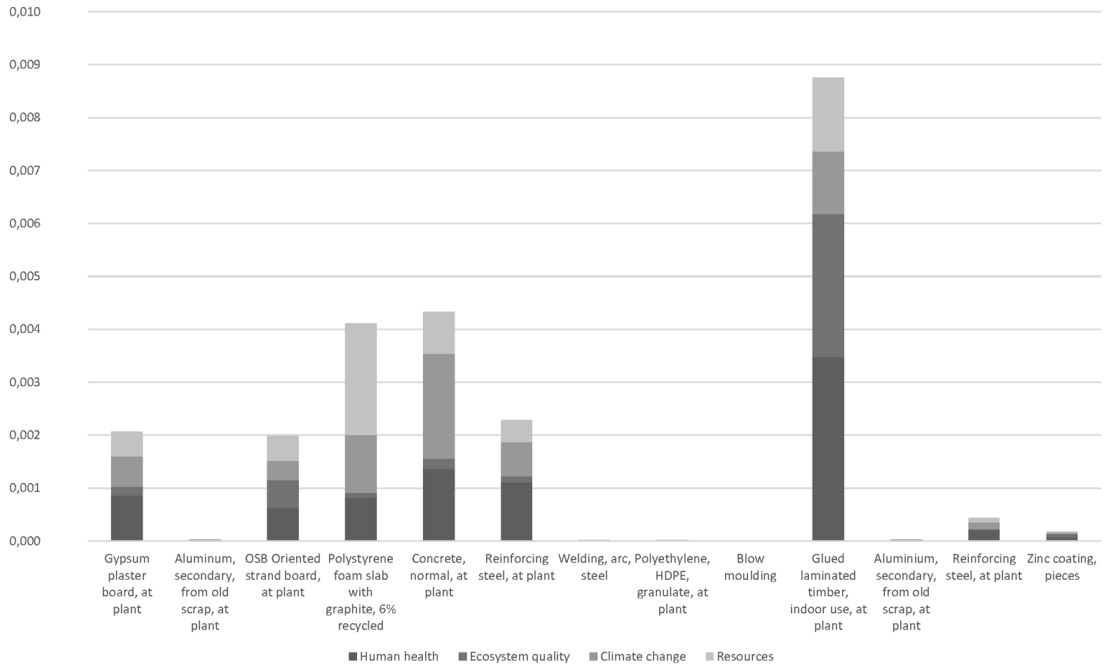

Figure 18. Diagram presenting the comparison of materials and operations impacts with the IMPACT 2002+ method.

The last calculation concerns the damage impact for each material and operations and an evaluation of output is given by a comparison between data (Table 6). In Human health category, OSB panel produces minimal impact while Glued laminated timber is responsible for the greatest weight on the environment because of the amount of the material and the processes. The most important damages of Glued laminated timber are due to the impact categories Respiratory inorganics (35.1%), Land occupation (18.8%), Non-renewable energy (15.9%), Global warming (13.5%) and Terrestrial ecotoxicity (11.5%). In Ecosystem quality, Glued laminated timber produces the greater impact due to the raw materials and processes utilized. In Climate change the assessment show lower values for OSB and Reinforcing steel, but the higher values are presented in the concrete panel because of clinker production. In Resources comparison of insulation foam and concrete is interesting. Total sum of impacts is quite similar and shows higher outcomes because of the higher volumes in the CGFP panel. Otherwise eco-points for Resources are very different due to the high consumption of non-renewable energy in the production of polystyrene foam slab.

Damage category	Human health [pt m^{-2}]	Ecosystem quality [pt m^{-2}]	Climate change [pt m^{-2}]	Resources [pt m^{-2}]	Total [pt m^{-2}]
Gypsum plaster board, at plant/CH U	0.00086263	0.00016832	0.00056327	0.00046753	0.00206175
Aluminium, secondary, from old scrap, at plant/RER U	0.00001089	0.00000240	0.00001234	0.00000686	0.00003249
Oriented strand board, at plant/RER U	0.00061737	0.00053710	0.00036376	0.00046039	0.00197861
Polystyrene foam slab with graphite, 6% recycled {GLO}| market for | Alloc Def, U	0.00081505	0.00009442	0.00109508	0.00210795	0.00411250
Concrete, normal, at plant/CH U	0.00135403	0.00019873	0.00198625	0.00078793	0.00432694
Reinforcing steel, at plant/RER U	0.00111175	0.00011530	0.00063626	0.00041956	0.00228289
Welding, arc, steel/RER U	0.00001063	0.00000294	0.00000355	0.00000300	0.00002014
Polyethylene, HDPE, granulate, at plant/RER U	0.00000387	0.00000010	0.00000316	0.00000878	0.00001591
Blow moulding/RER U	0.00000354	0.00000044	0.00000235	0.00000257	0.00000891
Glued laminated timber, indoor use, at plant/RER U	0.00347911	0.00270095	0.00118043	0.00139273	0.00875323
Aluminium, secondary, from old scrap, at plant/RER U	0.00001089	0.00000240	0.00001234	0.00000686	0.00003249
Reinforcing steel, at plant/RER S	0.00020929	0.00002171	0.00011978	0.00007898	0.00042975
Zinc coating, pieces/RER U	0.00006893	0.00006154	0.00002436	0.00002275	0.00017758
Total	**0.00855799**	**0.00390638**	**0.00600292**	**0.00576589**	**0.02423318**

Table 6. Evaluation of the comparison of the impact for damage category of materials with IMPACT 2002+ method.

Finally the environmental impact of CGFP configuration is summarized in the total value of 0.02456 eco-points for square meters (pt m^{-2}); the involved processes affect particularly the Human health damage category, corresponding to 0.00856 eco-points for square meters (35%), while other damages show lower impact: 0.00391 eco-points for square meters (16%) for Ecosystem quality, 0.00600 eco-points for square meters (25%) for Climate change, 0.00577 eco-points for square meters (24%) for Resources.

The performed analyses allow also to evaluate the environmental impacts of basic configuration of CGFP from the point of view of Embodied Energy (919.44 MJ m^{-2} or 2766 MJ m^{-3}) and Carbon Footprint (60.63 kg CO_2eq m^{-2} or 254.65 kg CO_2eq).

Embodied Energy is defined as the total energy used during the life-cycle of products: raw material extraction, transportation, manufacture. In the evaluation of the damage category impact, Resource category shows values about non-renewable energy and mineral extraction, that is precisely the Embodied Energy: graphics below (Table 7) shows how each compartment of energy consumption has different amount and weight for each considered process (Figure 19).

	Non-renewable energy [MJ m^{-2}]	Mineral extraction [MJ m^{-2}]	Total [MJ m^{-2}]
Gypsum plaster board, at plant	70,92	0,14	71,05
Aluminum, secondary, from old scrap, at plant	1,02	0,03	1,04
OSB Oriented strand board, at plant	69,67	0,30	69,97
Polystyrene foam slab with graphite, 6% recycled	363,47	0,05	363,53
Concrete, normal, at plant	119,39	0,36	119,75
Reinforcing steel, at plant	61,01	2,76	63,76
Welding, arc, steel	0,43	0,02	0,46
Polyethylene, HDPE, granulate, at plant	1,33	0,00	1,33
Blow moulding	0,39	0,00	0,39
Glued laminated timber, indoor use, at plant	210,93	0,73	211,66
Aluminium, secondary, from old scrap, at plant	1,02	0,03	1,04
Reinforcing steel, at plant	11,48	0,52	12,00
Zinc coating, pieces	3,16	0,29	3,46
Total Embodied Energy	914,22	5,23	919,44

Table 7. Results for calculation f Embodied Energy according to IMPACT 2002+ method.

The assessment of process shows how the greater environmental impacts regard the insulation material, that affects almost the 18 % of total impact (corresponding to a 0.0044 pt m^{-2}): the values are quite similar to concrete slab impact, but, while concrete is a component with optimized characteristics in structural and formal terms, insulation material should be considered as a component that could be substituted on this CGFP configuration. For this reason, the research project has developed a deeper study that compares some alternative solutions of the inner insulation materials in order to promote alternative design (e.g. a minor thickness allows more space for system) and with the aim to reduce the general environmental impacts [81].

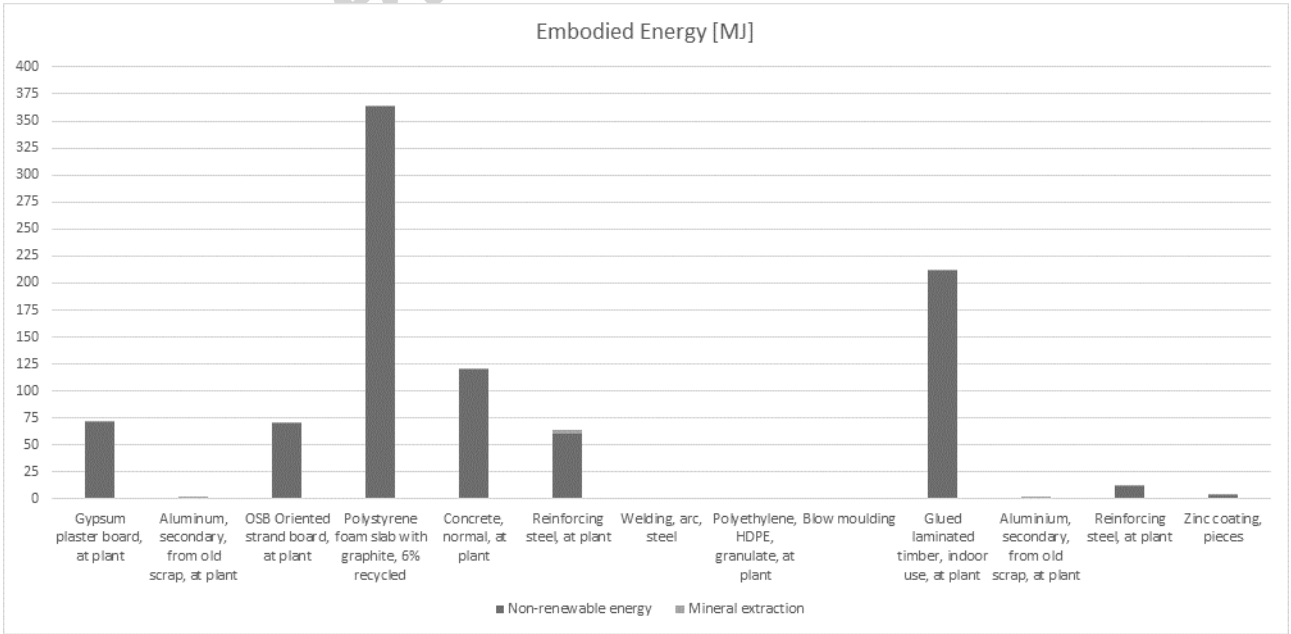

Figure 19. Results for calculation f Embodied Energy according to IMPACT 2002+ method.

A Carbon Footprint is an environmental index and is historically defined as "the total sets of greenhouse gas emissions caused by an organization, event, product or individual": it measures the impact that these emissions have on climate change to anthropogenic. The carbon footprint is expressed in equivalent carbon dioxide, which value indicates the level of the GWP (Global Warming Potential) of greenhouse gases, or rather their global warming potential for each selected material. A comparison between the production process of packages is developed according to the method 2013 IPCC (Intergovernmental Panel on Climate Change), that lists the climate change factors of IPCC with a timeframe of 20, 100 and 500 years: unit value is attributed on-base percentage to the material with higher equivalent carbon dioxide and the remaining values were consequently obtained.

Comparing with the environmental assessment of other precast panels, the state of the art on similar research reports how environmental assessment for buildings depends on the materials, the different technology and the process management adopted [82, 83, 84]. For example, in Fu et al. [85], the use of timber frame could achieve a reduction of carbon emissions: the masonry wall made of bricks and blocks is replaced with timber frame without intervening into structure and insulation partition; the wall partition in timber frame installed in the case study produced a lighter weight and reduces the 16% of carbon emission quantity (approximately 363 kg CO_2 per m^2 of floor). Moreover, the materials used in the building could allow a carbon reduction of the applied substructure, providing also additional benefits: reduced earthworks, less spoil and less export off site for waste material.

Focusing on the choice of materials, the assessment shows that high weight on the impacts is given by the choice of insulation foam, but the values of EPS foam are similar in the study of Tingley et al. [86], that shows how the expanded polystyrene achieves the lowest environmental

impact in the most of impact categories examined in comparison to other kind of insulation material.

The analysis environmental impact in CGFP panel confirms the results given by the case study in Aye et al. [87]: analysing three scenarios with precast elements, the constructions in timber and concrete reveal a lower embodied energy values because there is a less exploitation of energy intensive process with respect to a steel construction. Moreover, focusing on the external wall component, CGFP configuration shows a quite similar structure in timber frame that includes insulation materials and finish layers, but embodied energy values are lower and comparable in respect to the external wall (1971,8 MJ m^{-2}) in this study, so the general trend of breakdown energy is confirmed and very low.

Another comparison is given by the Australian National Timber Development Council document [87] that listed embodied energy values for common building elements; for external wall in timber frame, brick veneer covered, including internal insulation, values are very similar (1060 MJ m^{-2}) and the main difference lays in the fact that CGFP panel is precast and includes other processes.

In Čuláková et al. [88], a multi-criteria analysis of material selection shows how to decrease environmental impacts by the use of alternative solutions from renewable materials: the scenario with massive cross laminated timber (CLT) panel and wood-fiber insulation is very interesting because at equal thermal properties (0.11 W $m^{-2}K^{-1}$) the outcomes give very similar to CGFP panel in terms of embodied energy (1089.940 MJ m^{-2}) and carbon footprint (-81.094 kg CO_2eq m^{-2}).

6. Conclusions

Through the results on structural, thermal and sustainability performances of the CGFP system presented in this research the following conclusions can be drawn:

- despite the complexity of the tested system the experimental results match the numerical one with good approximation. The failure mechanism that best approximates the strength of panel Set 0 is the racking mode with a coefficient of variation between experimental and analytical maximum

load less than 7% for two tests and equal to 21 % for the other one. The FE analysis finds the best correlation between experimental and numerical results above all for the test 1 both for the maximum load and maximum displacement with a variation by 1% and 3% respectively. This variation increases over 14% for test 1 and 2;

- the deformation involves the elastic and inelastic behaviour assuring a global dissipative capacity through the progressive strengthening response of the external connectors and the plastic deformation capacity of internal connections. The failure under shear mechanism can be described by bi-linear F-Δ analytical response curve;

- the thermal transmittance presents very low value (0.20 W m^{-2} K^{-1}) in both analyzed configurations, and the construction systems shows dispersion effects by the thermal bridges that are comparable to similar situation in traditional construction systems;

- the single modular panels offer several advantages in the sustainability field. A great flexibility and speed in production and transport is given by the possibility to divide the RC slab from the glulam frame;

- the CGFP panel presents a low level of impacts in respect to similar studies in term of environmental assessment an embodied energy. LCA is a tool able to support the actions to improve the environmental management of its production process. After identifying the stages (such as Resources and Human health) on which a reduction of the environmental impact of the product is get involved, then it is possible to reduce also the consumption of energy, raw materials and the production of waste, consequently reducing the production costs. However, it is necessary to emphasize that the models used for the analysis of inventory are limited by the assumptions that are implicitly contained in them.

Acknowledgements

The authors thank Montini Enterprise (http://montinicase.it) that produced the CGFP system and funded the research program. The tests were carried out in the facilities of the Laboratories of

Strength of Materials (LabSCo) and of Building Physics (FisTec) at IUAV University of Venice.

Thanks to Stefano Fortuna for the collaboration to life cycle assessment.

References

1. L. Pozza, *Ductility and behaviour factor of wood structural systems*, PhD thesis, University of Padova, 2013.
2. R. Destro, G. Boscato, U. Mazzali, S. Russo, F. Peron, P. Romagnoni, Structural and thermal behaviour of a timber-concrete prefabricated composite wall system, *6th International Building Physics Conference, IBPC 2015; Torino; Italy, 14-17 June 2015*, 78, 2730-2735.
3. G. Boscato, A. dal Cin, R. Destro, Structural Behaviour and Comparison of CGF Panels, *Advanced Materials Research*, 900, 2014, 463-467.
4. F.E Richart and C.B. Williams, Tests of composite timber-concrete beams.“ Journal oft he American Concrete Institute 14(4), 253-276, 1943
5. P. Muller, Decke aus hochkantig stehenden Holzbohlen oder Holzbrettern und Betondeckschicht, Patentschau aus dem Betonbau und den damit verwandten Gebieten, Auszuge aus den Patentschriften, *Beton und Eisen*, H. XVII, S. 244, 1922 (in German).
6. DTFHA (2016). National Bridge Inventory (BBI), DTFHA 2016
7. C.M. Cone, A composite timber-concrete bridge.“ TDA Bulletin, 1(9), 1963
8. G. Nolan, Experience with concrete overlayed bridges in Tasmania. http://oak.arch.utas.edu.au/research/bridge/sem2.asp (4 Nov., 2009).
9. R. Pischl and G. Schickhofer, The Mur River wooden bridge, Austria.“ Structural Engineering International 3(4), 217-219, 1993.
10. J. Natterer, T. Herzog and M. Volz, Built in timber 2, Presses polytechniques et universitaires romandes, Lausanne, Switzerland, 1998
11. E. Aasheim, Development of timber bridges in the Nordic countries, Proc. Of the 6th World Conference on Timber Engineering, Vancouver, Canada, 2000
12. M. Flach, and C.D. Frenette, Wood-concrete-composite-technology in bridge construction, Proc. Of the 8th World Conference on Timber Engineering, Lahti, Finland, 289-294, 2004.
13. C.A. Weaver, W.G. Davids and H.J. Dagher, Testing and analysis of partially composite fiber-reinforced polymer-glulam-concrete bridge girders, Journal of Bridge Engineering 9(4), 316-325, 2004
14. J. Balogh, N. Miller, M. Fragiacomo and R. Gutkwoski, Time-dependent behavior of composite wood-concrete bridges made from salvaged utility poles, Proc. of the 11th World Conference on Timber Engineering, Trentino, Italy, 2010
15. A. Parisi, M. Piazza, Restoration and Strengthening of Timber Structures: Principles, Criteria, and Examples. Structural Design and Construction, Volume 12, Issues 4, November 2007.
16. L. Bathon, O. Bletz, R. Bahmer, Concrete bearings - a new design approach in wood-concrete-composite applications, Proc., 10th World Conf. on Timber Engineering, Portland, OR, 2006.
17. M. Flach, F. Schaonborn, *Prefabricated wood-concrete Slabs*, Universität Innsbruck, Austria, 2006.
18. R. Crocetti, M. Flansbjer, Timber-concrete composite structures with prefabricated FRC slab, *Proceedings of 11th World Conference of Timber Engineering (11 WCTE)*, Riva del Garda (Italy), 2010.
19. R. Crocetti, T. Sartori, R. Tomasi, Innovative Timber-Concrete Composite Structures with Prefabricated FRC Slabs, Journal of Structural Engineering, Vol. 141, No. 9, 04014224, 2015.
20. E. Lukaszewska, H. Johnsson and L. Sthen, Connections for prefabricated timber-concrete composite systems.” Proc., World Conf. on Timber Engineering, 2006.

21. E. Lukaszewska, Development of prefabricated timber-concrete composite floors. Ph.D. thesis, Div. of Structural Engineering, Dept. of Civil, Mining, and Environmental Engineering, Luleå Univ. of Technology, Luleå, Sweden, 2009
22. R. Gutkowski, K. Brown, A. Shigidi and J. Natterer, Laboratory tests of composite wood–concrete beams, Construction and Building Materials, 22(6), 1059-1066, 2008.
23. N.T. Mascia, J. Soriano, Benefits of timber-concrete composite action in rural bridges, Materials and Structures 37(2), 122-128, 2004.
24. J. C. Molina, C. Calil Jr, Dynamic analysis on glued steel bar connectors for composed log-concrete deck bridges, Proc. of the 10th World Conference on Timber Engineering, Miyazaki, Japan, 2008.
25. R. Astori, R. Barrios D'Ambra, F. Solari, L. Kosteski, Numerical-experimental analysis of a composite timber-concrete section, Mecánica Computacional, XXVI, 111-128, 2007.
26. M.F. Benitez, Development and testing of timber/concrete shear connectors, Proc. of the 6th World Conference on timber engineering, Vancouver, Canada, 2000.
27. A. Simon, W. Haedicke, J. Mueller, K. Rautenstrauch, Development of a new connector type for Hybrid timber bridges, Proc. of the 10th World Conference on Timber Engineering, Miyazaki, Japan, 2008.
28. J. Tommola, L. Salokangas, A. Jutila, Test on Shear Connectors, Nordic Timber Council, Stockholm, Sweden, 1999.
29. J. Miotto, A. Dias, Glulam-concrete composite structures: Experimental investigation into the connection system, Proc. of the 10th World Conference on Timber Engineering, Miyazaki, Japan, 2008
30. R. Mäkipuro, J. Tommola, L. Salokangas, A. Jutila, Wood-Concrete Composite Bridges, Nordic Timber Council, Stockholm, Sweden, 1996.
31. P. Yttrup, Concrete and timber composite construction for enhanced strength, stiffness and service life for timber bridges, http://oak.arch.utas.edu.au./research/bridge/sem3.asp (2009)
32. P. Aldi, U. Kuhlmann, Fatigue strength of timber-concrete composite bridges: Determination of a S-N-line for the grooved connection and the "X-connectors, Proc. of the 11th World Conference on Timber Engineering, Trentino, Italy, 2010.
33. L. Bathon, O. Bletz, Long term performance of continuous wood-concrete-composite systems, Proc. of the 9th World Conference on timber engineering, Portland, USA, 2006
34. M. Brunner, M. Romer, M. Schnüriger, Timber-concerte-composite with an adesive connector (wet on wet process), Materials and Structures 40(1), 119-126, 2007.
35. R. Le Roy, H.S. Pham, G. Foret, New wood composite bridges, EuropeanJournal of Environmental and Civil Engineering 13(9), 1125-1139, 2009.
36. O. Ben Mekki, F. Toutlemonde, Experimental validation of a 10-m-span composite UHPFRC-carbon fibers-timber bridge concept. "Journal of Bridge Engineering 16(1), 148-157, 2011.
37. S. Nakamura, P. Collin, Steel concrete composite structures: Introduction, Struct. Eng. Int., 19(4), 395–395, 2009
38. P. Collin, A. Stoltz and M. Möller, Innovative prefabricated composite bridges, Proc., Int. Association for Bridge and Structural Engineering (IABSE) Symp. Rep., Zurich, Switzerland, 2002.
39. A. Jutila, L. Salokangas, Wood-concrete composite bridges - finnish speciality in the Nordic countries." Proc., Int. Conf. on Timber Bridges, 2010.
40. C. Loss, M. Piazza, D. Zonta, Seismic design of timber building with a direct displacement-based design method, *Proceedings of the 2nd International Conference on Structures and Architecture*, Guimaraes (Portugal), 2013.
41. L. Pozza e R. Scotta, *Seismic behaviour of wood-concrete frame shear wall system and comparison with code provisions*, ICRIBC Working Commission W18 - Timber Structures, 2010.
42. D. Yeoh, M. Fragiacomo, M. De Franceschi, K. H. Boon, State of the Art on Timber-Concrete

Composite Structures: Literature Review, J. Struct. Eng., 2011, 137(10), 1085-1095.
43. J.N. Rodrigues, A.M.P.G. Dias, P. Providencia, Timber-Concrete Composite Bridges: State-of-the-Art Review, Bioresources, 2013, 8, 6630-6649.
44. EU (2010) European Commission -Energy efficiency: delivering the 20% target
45. Directive 2012/27/UE on energy efficiency, amending Directives 2009/125/EC and 2010/30/EU and repealing Directives 2004/8/EC and2006/32/EC, *Official Journal of the European Union*, 55, 2012, 1–56.
46. C.E.J. Martins, P. Santos, P. Almeida, L. Godinho, A.M.P.G. Dias, Acoustic performance of timber and timber–concrete floors, *Construction and Building Materials*, 101, 2013, 684-691.
47. J. O'Neill, D. Carradine, P. Moss, M.R.D. Fragiacomo, A. Buchanan, Design of timber–concrete composite floors for fire resistance, *J. Struct. Fire Eng.*, 2(3), 2011, 231–242.
48. A. Dodoo, L. Gustavsson, R. Sathre, Effect of thermal mass on life cycle primary energy balances of a concrete- and a wood-frame building, *Appl. Energy*, 92, 2012, 462–472.
49. S. Thiers, B. Peuportier, Energy and environmental assessment of two high energy performance residential buildings, *Building and Environment*, 51, 2012, 276–284.
50. L. Jaillon, C.S. Poon, Y.H. Chiang, Quantifying the waste reduction potential of using prefabrication in building construction in Hong Kong, *Waste Management*, 29(1), 2009, 309–320.
51. R. J. Cole, Energy and greenhouse gas emissions associated with the construction of alternative structural systems, *Building and Environment*, 34(3), 1997, 335–348.
52. A. Filiatrault, H. Isoda, B. Folz, Hysteretic damping of wood framed buildings, *Engineering Structures*, 25, 2003, 461-471.
53. G.C. Foliente, Hysteresis modelling of wood joints and structural system, *Journal of Structural Engineer (ASCE)*, 121(6), 1995, 1013-1022.
54. P.J. Judd, F.S. Fonseca, Analytical model for sheating-to-framing connections in wood shear walls and diaphragrams, *Journal of Structural Engineering*, 131(2), 2005, 345-352.
55. W. Pang, D.V. Rosowsky, Direct displacement procedure for performance-based seismic design of mid-rise woodframe structures, *Earthquake Spectra*, 25 (3), 2009, 583-605.
56. M. Popovski, E. Karacabeyli, Seismic behaviour of cross-laminated timber structures, *Proceedings of the 12th World Conference on Timber Engineering (12WCTE)*, Auckland (New Zealand), 2012.
57. M.J.N. Priestley, G.M. Calvi, M.J. Kowalsky, *Direct Displacement-based seismic design*, IUSS Press, Pavia (Italy), 2007.
58. C. Loss, *Displacement-Based seismic design of timber structures*, PhD thesis, University of Trento, 2011.
59. S. V. Glass et al., Moisture relations and physical properties of wood, *Wood Handbook*, 2010.
60. H. U. A. Ge and F. Tariku, Evaluation of the thermal performance of innovative pre-fabricated wall systems through field testing, *Proceedings of Building Enclosure Science & Technology (BEST3) Conference*, Atlanta (USA), 2012.
61. K. Mahapatra and S. Olsson, Energy Performance of Two Multi-Story Wood-Frame Passive Houses in Sweden, *Buildings*, 5(4), 2015, 1207–1220.
62. I. Kildsgaard, A. Jarnehammar, A. Widheden, M. Wall, Energy and environmental performance of multi-storey apartment buildings built in timber construction using passive house principles, *Buildings*, 3, 2013, 258–277.
63. M. Kalousek, D. Bečkovský, Thermal comfort of lightweight building in summer time, *Proceedings of the 8th International Conference on Healthy Buildings*, Lisboa (Portugal), 2006, 64–67.
64. T. O. Adekunle and M. Nikolopoulou, Thermal comfort, summertime temperatures and overheating in prefabricated timber housing, *Building and Environment*, 103, 2016, 21–35.
65. I. Skotnicová, Z. Galda, P. Tymova, L. Lausova, Experimental Measurements and Numerical Simulations of Dynamic Thermal Performance of External Timber Frame Wall, *Adv. Mater.*

Res., 899, 2014, 126–130.
66. ISO 14040, 2006 *Environmental Management: Life Cycle Assessment Principles and Framework*, Internation Standards Organisation, Paris, 2006.
67. L. Aye, T. Ngo, R. H. Crawford, R. Gammampila, P. Mendis, Life cycle greenhouse gas emissions and energy analysis of prefabricated reusable building modules, *Energy and Buildings*, 47, 2012, 159–168, doi:10.1016/j.enbuild.2011.11.049.
68. C. D. Frenette, C. Bulle, R. Beauregard, A. Salenikovich, D. Derome, Using life cycle assessment to derive an environmental index for light-frame wood wall assemblies, *Building and Environment*, 45(10), 2010, 2111–2122.
69. G. P. Gerilla, K. Teknomo, and K. Hokao, An environmental assessment of wood and steel reinforced concrete housing construction, *Building and Environment*, 42(7), 2007, 2778–2784.
70. A. Pérez-García, A. G. Víllora, G. G. Pérez, Building's eco-efficiency improvements based on reinforced concrete multilayer structural panels. *Energy and Buildings*, 85, 2014, 1–11. doi:10.1016/j.enbuild.2014.08.018.
71. C. Martins, A. M. P. G. Dias, R. Costa, P. Santos, Environmentally friendly high performance timber-concrete panel, *Constr. Build. Mater.*, 102, 2016, 1060–1069.
72. *Eurocode 5: Design of timber structures. Part 1-1: General – Common rules and rules for buildings*, European Committee for Standardization, 2004, Bruxelles (Belgium).
73. UNI EN 594, *Timber structures. Test methods. Racking strength and stiffness of timber frame wall panels*, 2011.
74. ISO 8990, *Thermal insulation, Determination of steady-state thermal transmission properties: Calibrated and guarded hot box*,1994.
75. T. Kalamees, J. Vinha, Hygrothermal calculations and laboratory tests on timber-framed wall structures, Building and Environment, 38(5), 689–697, 2003.
76. *Using Strand 7 Introduction to the Strand7 finite element analysis system*, Strand7 Pty Ltd., Sydney (Australia), 2016.
77. M. Goedkoop, M. Oele, J. Leijting, T. Ponsioen, E. Meijer, *Introduction to LCA with SimaPro*, Prè (Product Ecology Consultants), Amersfoort (The Netherlands), 2016.
78. B. P. Weidema, C.Bauer, R. Hischier, C. Mutel, T. Nemecek, J. Reinhard, C.O. Vadenbo, G. Wernet, *Overview and methodology, Data quality guideline for the ecoinvent database version 3*, Swiss Centre for Life Cycle Inventories, St. Gallen (Switzerland), 2016.
79. S. Humbert, A. De Schryver, X. Bengoa, M. Margni, O. Jolliet, *IMPACT 2002+: User Guide*, Quantis Sustainability Counts, Lausanne (Switzerland), 2012.
80. O. Jolliet, M. Margni, R. Charles, IMPACT 2002+: A new life cycle impact assessment methodology, *International Journal of Life Cycle Assessment*, 8(6), 2003, 324-330.
81. S. Fortuna, T. Dalla Mora, F. Peron, P. Romagnoni, Environmental Performances of a Timber-concrete Prefabricated Composite Wall System, Energy Procedia, 113, 90-97, 2017.
82. J. Monahan, J. C. Powell, An embodied carbon and energy analysis of modern methods of construction in housing: A case study using a lifecycle assessment framework, *Energy and Buildings*, 43(1), 2011 , 179–188, doi:10.1016/j.enbuild.2010.09.005.
83. B. Venkatarama, K. Jagadish, Embodied energy of common and alternative building materials and technologies, *Energy and Buildings*, 35(2), 2003, 129–137, doi:10.1016/S0378-7788(01)00141-4.
84. A. B. Robertson, F. C. F. Lam, R. J. Cole, A Comparative Cradle-to-Gate Life Cycle Assessment of Mid-Rise Office Building Construction Alternatives: Laminated Timber or Reinforced Concrete, *Buildings*, 2(3), 2012, 245–270, doi:10.3390/buildings2030245.
85. F. Fu, H. Luo, H. Zhong, A. Hill, Development of a Carbon Emission Calculations System for Optimizing Building Plan Based on the LCA Framework, *Mathematical Problems in Engineering*, 2014, 1-13, doi:10.1155/2014/653849.
86. D. Densley Tingley, A. Hathway, B. Davison, An environmental impact comparison of external wall insulation types, *Building and Environment*, 85, 2015, 182–189.

87. *Environmentally friendly housing using timber: principles*, Forest and Wood Products Research and Development Corporation, Brisbane (Australia), 2001.
88. M. Čuláková, V. Vilčeková, J. Katunská, E. Krídlová Burdová, Multi-Criteria Analysis of Material Selection in order to Reduction of Environmental Impacts, *Chemical Engineering Transactions*, 35, 2013, 379–384, doi: 10.3303/CET1335063.

Highlights

- The paper resumes and completes results of a three years investigation on the structural, thermal and environmental performances of a concrete-glulam prefabricated composite wall system.
- The strength and stiffness of concrete-glulam prefabricated panels have been investigated by load-displacements tests;
- thermal performance was analyzed matching values given by numerical simulations and experimental tests executed by hot box apparatus.
- The environmental impacts of the system is verified defining its Carbon Footprint and Embodied Energy by using the life cycle assessment method